Mixed Convection Heat Transfer In a Vertical Channel With different shapes of Protrusions at Walls

A Thesis submitted

In Partial Fulfilment of the Requirements
for the Degree of

Master of Engineering in Automobile Engineering

By

Sumit Kumar

REGISTRATION NO- 154355

EXAMINATION ROLL NO- M4AUT22022

CLASS ROLL NO- 002011204022

UNDER THE GUIDANCE OF

PROF. SANDIP SARKAR

JADAVPUR UNIVERSITY

DEPARTMENT OF MECHANICAL ENGINEERING
FACULTY OF ENGINEERING & TECHNOLOGY
JADAVPUR UNIVERSITY 188, RAJA S.C. MULLICK ROAD,
KOLKATA-700032, INDIA

JUNE, 2022

DECLERATION OF ORIGINALITY AND COMPLIANCE OF ACEDEMIC ETHICS

I hereby declare that the thesis entitled **"Mixed Convection Heat Transfer in a Vertical Channel with Different Shapes of Protrusions at Walls"** contains literature survey and original research work by the undersigned candidate, as a part of his MASTER OF ENGINEERING IN AUTOMOBILE ENGINEERING studies during academic session 2020-2022. All information in this document have been obtained and presented in accordance with the academic rules and ethical conduct. I also declare that, as required by these rules of conduct, I have fully cited and referenced all the material and results that are not original to this work.

Name: Sumit Kumar

Class Roll Number: 002011204022

Examination Roll Number: M4AUT22022

University Registration Number: 154355 of 2020-21

Thesis Title: **Mixed Convection Heat Transfer in a Vertical Channel with Different Shapes of Protrusions at Walls**

Date: _____

Signature: _____

CERTIFICATE OF RECOMMENDATION

This is to certify that the thesis entitled "**Mixed Convection Heat Transfer in a Vertical Channel with Different Shapes of Protrusions at Walls**" is a bonafide work carried out by Sumit Kumar under our supervision and guidance in partial fulfilment of the requirements for awarding the degree of Master of Engineering in Automobile Engineering under Department of Mechanical Engineering, Jadavpur University during the academic session 2020-2022.

Prof. Sandip Sarkar

Professor

Department of Mechanical Engineering
Jadavpur University, Kolkata

Prof. Amit Karmakar

Head of Department

Department of Mechanical Engineering
Jadavpur University, Kolkata

Prof. Chandan Mazumdar

Dean

Faculty Council of Engineering and Technology

Jadavpur University, Kolkata

CERTIFICATE OF APPROVAL*

The foregoing thesis, entitled "Mixed Convection Heat Transfer in a Vertical Channel with Different Shapes of Protrusions" is hereby approved as a creditable study in the area of Microfluidics carried out and presented by **Mr. Sumit Kumar (Registration No. 154355 of 2020-21)** in a satisfactory manner to warrant its acceptance as a prerequisite to the degree for which it has been submitted. It is notified to be understood that by this approval, the undersigned do not necessarily endorse or approve any statement made, opinion expressed and conclusion drawn therein but approve the thesis only for the purpose for which it has been submitted.

Final Examination for Evaluation of the Thesis

Board of Members

---------- ----------

---------- ----------

---------- ----------

*Only in case the thesis is approved

ACKNOWLEDGEMENTS

I would like to express my sincere and heartiest gratitude to my supervisor Prof. Sandip Sarkar for always having my back and showing me the right path to carry out this research work. He gave me confidence and filled me with enthusiasm regarding this research work. It was during our first discussion I was introduced to “Mushroom Shape of Protrusions” for the “first time” and the way he explained the research area caught my attention and interest and it’s been more than a year since then and I thoroughly enjoyed what I did. I had always looked forward towards research as having the perfect balance between studies and enjoying life and I enjoyed the work-life balance under his guidance to the fullest. I am also thankful to him for providing me with support and assistance in every possible way and most importantly the friendly companionship we shared. I hardly had to wait a day before getting help from Sir which I had asked for in priority.

I would also like to mention my **Parents**, my senior **Joy Mondal**, my friends (Lab Partner) **Piyush Shaw and Raushan Kumar** and special thanks to my friend **Sanjana Ranjan** as their never-ending support and wholehearted helps are the real impetus to produce my best.

SUMIT KUMAR
Jadavpur University

Date: _____

ABSTRACT

Mixed Convection Heat Transfer in a vertical channel with different shapes of protrusions at wall have been numerically investigated using air as a working medium. The, shape of the protrusions at walls are rectangular, triangular or combination of both and Mushroom Shape of protrusions.

The significance of this research work primarily from several associated engineering applications, including cooling of electric and electronic equipment, nuclear reactor fuel elements, home ventilation, and many more.

The channel is formed by two vertical parallel walls having constant temperature and protrusions are situated at these walls. There are six number of protrusions on the left wall and five number of protrusions on the right wall. The flow is assumed to be two dimensional, transient, laminar, incompressible and gravity enabled. The finite volume method and the SIMPLE algorithm are used to solve the conservation equations of mass, momentum and energy during mixed convection.

The models are first verified by simulating the mixed convection on a vertically placed plate with single protrusion at wall and comparing the results with literature. It is observed that the present results agree very well with results of the experimental studies. In present work, it is observed that for Mushroom shape of protrusions, wall heat flux is maximum because more surface area is available and also, blockage of fluid is more than other shape of protrusions. For a particular Re and Pr, wall heat flux is maximum for Mushroom Shape of protrusions and it's value increases as we increases Re and Pr.

Keywords: Mixed Convection, Vertical Channel, Mushroom Protusions, Wall Heat Flux, Heat Transfer co-Efficient

Contents

List of Figures

Figure Page No.

Dedicated to

My

Parents

Chapter 1

Introduction

1.1 General Description

Many engineering applications result in the creation of heat as a by-product. This often undesirable by-product has the potential to lower system performance. Because it has real-world engineering uses including cooling electronic components, internal cooling systems for gas turbine blades, and solar panels, the study of mixed convection flow via channels is crucial. Therefore, by employing various techniques for heat dissipation away from the system, many engineering systems attempt to prevent this overheating issue as much as feasible. Protrusions are one of the simplest and cheapest ways to dissipate excess heat, and they have been effectively employed in several technical applications. In order to keep the component below the permissible limits, fluid velocity must be increased as the component dissipates more heat than the cooling system can handle. The creation of buoyancy due to temperature differences generates fluid flow in both forced and free convection. Although the pushed flow can go in any direction, the buoyancy force only operates vertically. The forced flow in vertical internal flows can be either upward or downward, and the fluid inside the conduit can either receive heat from or be heated by it. The study of fluid flow and heat transfer properties with a moving plate in a channel is also important because it has many practical applications, including rolling, extrusion, continuous casting, and melt spinning etc. The present study would be extremely helpful because the quality of the product is mostly dependent on the temperature distribution and flow parameters.

The heat transfer coefficient and the surface area of the fins determine how quickly heat is dissipated from a fin design by convection heat transfer. Also, we can increase wall heat flux, q by using fans to force the fluid to flow over the fins. However, this choice is more expensive. In order to improve the overall heat transfer from the protrusions, by adding more fins to the base material, the surface area of the fins can also be increased. However, it is important to note that increasing the number of protrusions also reduces the space between the neighbouring fins, therefore the number of fins should be optimised. This might result in boundary layer interference and air flow resistance, which would lower the efficiency of the heat transfer.

1.2 Dimensionless Numbers

It is necessary to highlight a few dimensionless numbers that are frequently employed for the heat transfer phenomena in vertical channel.

1. Reynolds number (Re):

The Reynolds number represents the ratio of the inertial forces to viscous forces in a fluid flow.

$$Re = \frac{VD}{v}$$

Where, V is velocity of fluid, D is hydraulic diameter and v is Kinematic Viscosity of materials.

2. Prandtl number (Pr):

The Prandtl number is the ratio of the momentum diffusivity to the thermal diffusivity. It depends on the properties of the fluid. It gives information about the thickness of the velocity and thermal boundary layer.

$$\mathrm{Pr} = \frac{\nu}{\alpha}$$

Where, ν is Kinematic Viscosity and α is thermal diffusivity.

3. Grashof number (Gr):

It is defined as the ratio of the buoyancy forces to viscous forces. It can describe flow regime in natural convection. It functions in free convection is similar to the Reynolds number as in forced convection.

$$Gr = \frac{g\beta(T_s - T_\infty)l^3}{v^2}$$

Where, g is acceleration due to gravity, β is Thermal volumetric expansion coefficient, T_s and T_∞ is Temperature of the surface and the fluid respectively, l is Characteristic length

4. Richardson number (Ri):

The Richardson number is used to determine if the convection phenomena is assisted or naturally produced. It characterizes the flow regime and it is a ratio of buoyancy forces to inertial forces.

$Ri = \frac{Gr}{Re^2}$ < 1, Forced Convection

$Ri = \frac{Gr}{Re^2}$ ≈ 1, Mixed Convection

$Ri = \frac{Gr}{Re^2}$ >> 1, Free Convection

1.3 Mixed Convection

When the pumping force is superimposed on the buoyancy force and the natural and forced convections are comparable, heat transfer is characterized as the combined natural and forced convection.

A dimensionless group, Richardson number ($Ri = \frac{Gr}{Re^2}$), gives a measure of the buoyancy force to inertial force ratio in mixed convective flow across a vertical plate as mentioned in previous section.

1.4 Literature review

Rao et al. [1] presented and quantitatively investigated a conjugate mixed convection caused by projecting heat-generating ribs affixed to substrates (printed circuit boards). With air as the working medium, parametric study are carried out by varying the heat generation based Grashof number in the range $10^4 - 10^7$ and the fan velocity based Reynolds number in the range 0-1500. Barletta et al. [2] were performed to investigate the mixed convection flow in a parallel plate vertical channel by taking into consideration the effect of viscous dissipation in the fully developed area. The two boundaries are maintained at either equal or different temperatures and are supposed to be isothermal. Ligrani et al. [3] presented work for a channel with a dimpled surface on one wall and protrusions (with the same forms as the dimples) on the opposite wall, both with and without, the flow structure features. Rao et al. [4] presented the findings of a numerical investigation of the mixed convection and surface radiation issue in a vertical parallel-plate channel with flush-mounted, discrete heat sources in each wall. Assuming identical disposition and heat generation of the ribs on each board, a channel with periodic boundary conditions in the transverse direction is considered for analysis. The governing equations are discretised using a control volume approach on a staggered mesh and a pressure correction method is employed for the pressure–velocity coupling. The solid regions are considered as fluid regions with infinite viscosity and the thermal coupling between the solid and fluid regions is taken into account by the harmonic thermal conductivity method. Barletta et al. [5] revisits the problem of fully developed mixed convection flow with frictional heat production in a vertical channel enclosed by isothermal plane walls of the same temperature. The two boundaries are considered as isothermal and kept either at equal or at different temperatures. The velocity field, the temperature field and the Nusselt numbers are obtained by a perturbation series method. Esfe et al. [6] studied about two heated obstacles are put on the bottom wall of a horizontal channel that is experiencing laminar mixed convection flow of Al_2O_3/water nanofluids. The governing equations are solved numerically using finite volume method and SIMPLER algorithm. . The results are shown for a wide range of key parameters in the problem, i.e. Richardson number, Rayleigh number and nanoparticles volume fraction. In addition, the effects of different aspect ratios of obstacles on average Nusselt number are examined. The findings elucidate that the difference between average Nusselt numbers obtained from the three sets of

thermophysical models does not exceed 3%. Zanchini et al. [7] analysed Laminar flow for the impact of viscous dissipation on fully developed mixed convection in a parallel plate vertical channel whose walls conduct heat to an external fluid. In the examined cases the velocity fiel, the temperature field and the Nusselt numbers are evaluated. Umavathi et al. [8] investigated mixed convective magneto hydrodynamic flow issue in a vertical channel including consideration of the impact of viscous and ohmic dissipations. The channel walls are maintained at equal or at different constant temperatures. The velocity field and the temperature field are obtained analytically. It is found that the viscous dissipation enhances the flow reversal in the case of downward flow while it counters the flow in the case of upward flow. Aung and Worku [9],Cheng et al. [10],Hamadah and Wirtz [11] examined mixed convection in a vertical channel with symmetric and asymmetric heating of the walls. Desrayaud et al. [12] studied Laminar natural convection in a system of parallel vertical channels with a single projecting heat module situated mid-height on a substrate of finite thickness. Both conditions of equal and of diferent reference temperatures of the external fluid are considered. Sarper et al. [13] examines the buoyancy-induced flow and heat transfer in a parallel plate channel with a heat source array in order to model an electronic package. Studies are done for heat source cases that are flush installed and those that protrude. m. Studies are conducted both for flush mounted or protruding heat source cases. Habchi and Acharya [14] presented numerical analysis of laminar mixed convection of air in a vertical channel with a partial rectangular obstruction on one channel wall is carried out. The blocked wall is supposed to be heated, whereas the other wall is either adiabatic (asymmetric heating) or heated (symmetric heating). The results show that the highest velocity in the asymmetrically heated channel occurs near the adiabatic wall for low values of $\frac{Gr}{Re^2}$. This peak swings towards the hot wall when $\frac{Gr}{Re^2}$ grows. Beyond the obstruction, reverse flow is expected. Temperature changes are modest in this reverse flow zone. With decreasing $\frac{Gr}{Re^2}$ values, the average Nusselt number in the blockage and pre-blockage zones rises. Hung et al. [15] investigated local/average natural convection heat transfer characteristics in vertical parallel plates with a two-dimensional rectangular rib, both quantitative measurements and qualitative flow visualisation are used heating with asymmetric isotlux. For an equivalently heated flat plate, the range of local modified Rayleigh number investigated is in the laminar regime, and the heat transfer characteristics in the downstream region of obstruction are similar to those in the turbulent regime. Mandal et al. [16] performed a computational analysis of mixed convective heat transfer

with surface radiation in a rectangular channel with heat spreaders attached to each heat source. Air is the working fluid, and the flow is constant, incompressible, and laminar. The characteristics such as substrate and heat spreader thickness, heat source and channel width, and distance between heat sources are fixed. The influence of Reynolds number, emissivity of the heat source, heat spreader and channel wall on the rate of heat transfer is studied. Boutina et al. [17] illustrated the laminar mixed convection air-cooling of two similar heat sources installed in an inclined duct to simulate electronic components. The conservation equations of mass, momentum, and energy were solved using the finite volume approach and the SIMPLER algorithm. The results reveal that the Reynolds number, channel inclination angle, heat source dimensions, and spacing between them all have a significant impact on the enhancement of heat transmission inside the channel. Sultan [18] investigated forced convection heat transfer in a horizontal channel with passive cooling and several projecting heat sources with a small aspect ratio. Perforated holes are staggeredly positioned in two rows in the channel's base between heat sources. Outside air is naturally withdrawn via the perforated holes when the temperature between heaters rises. Tandda [19] carried out experiment to obtain heat transfer data for natural convective air flow in vertical channels with one surface roughened by transverse square ribs and the opposite surface smooth. The ribbed side was subjected to uniform wall temperature conditions, whereas the smooth side remained unheated. Additional studies were conducted in vertical channels without ribs, using the same channel geometry and heat conditions as before. Kelkar et al. [20] investigated the buoyancy-induced flow develops quite quickly in densely packed arrays of circuit boards containing equally spaced hot components. The dependence of the characteristics of the fully developed natural convection flow on the type of imposed thermal boundary conditions is discussed. In the context of the flow through an insulated channel with heated blocks mounted on one of the walls, the mathematical formulation for periodically fully developed natural convection with thermally active through flow is described. This is a generalisation of the literature-available notion of fully developed natural convection between parallel plates subjected to homogeneous heat input. The discretization of the temperature field is affected by the split of the temperature field into a periodic part and a linearly variable part.

1.5 Objective of the Thesis

It aims to investigate the effect on mixed convection heat transfer, heat transfer co-efficient, Nusselt Number, Wall shear stress by different shape of protrusion present at the wall. Studies are performed by varying the shape of protrusions present on the wall like rectangular shape, triangular shape or combination of both and this paper is mainly focuses on wall having mushroom shape of protrusions having aspect ratio (length/radius of curvature) varies from 0.87 to 3.48. Understanding the flow and heat transfer properties of mixed convection flow is the objective of the current study.

For various values of the governing parameters, such as Reynold's number, Prandtl number and protrusions position, heat transfer and fluid flow inside the channel were evaluated. Nusselt numbers, plots of isotherms, streamlines at various Prandtl numbers and Reynold's numbers and profile plots for temperature and velocity at the exit and inlet planes were among the study's findings.

1.6 Outline of thesis

Different geometry of vertical channel with different shapes of protrusions is covered in Chapter 2.

The governing equation in dimensional and non- dimensional form of two-dimensional incompressible mixed convection flow is covered in Chapter 3.

Numerical methods is discussed in Chapter 4.

Results of mixed convection flow via vertical channel are discussed in Chapter 5.

Chapter 2

Geometry and Computational Domain

2.1 Physical System

The geometry of the channel is formed by the two vertical plates with height 30H, and the distance between the plates is also same as height 30H. Both the walls are isothermal with different shapes of protrusions present at walls and flow has been allowed through this channel. The left plate has six protrusions and right plate has five protrusions.

In case of Rectangular Protrusions, Triangular Protrusions and combination of both, Width b and height h of vertical channel and different parameter of protrusions like Length L, thickness t and distance between two protrusions λ is given in the term of dimensionless parameter. So,

Length and width of channel is **b = h = 30H,**

Length of different protrusions are

$$\boldsymbol{L_1 = H,\ L_2 = 4H,\ L_3 = H, L_4 = 2H, L_5 = 3H, L_6 = 2H, L_7 = 2H,\ L_8 = 3H, L_9 = H,\ L_{10} = 4H,\ L_{11} = 2H}$$

Gap between two protrusions are given according to relation

$$\boldsymbol{\lambda_{0-1} = H,\ \lambda_{1-2} = \lambda_{2-3} = 2H,\ \lambda_{3-4} = \lambda_{4-5} = 4H,\ \lambda_{5-6} = 5H,\ \lambda_{0-7} = 4H,\ \lambda_{7-8} = 3H,\ \lambda_{8-9} = 6H,\ \lambda_{9-10} = 5H,\ \lambda_{10-11} = 4H}$$

Thickness of protrusions are **t = H.**

In case of Mushroom Shape of Protrusions, Size of the mushroom is defined by Aspect Ratio A, length l of respective mushroom is same as length of previous protrusions (rectangular, triangular or, combination of both).

Aspect Ratio (A) = $\frac{l}{r}$ where l is length of protrusions and r is radius of curvature of curved part.

Here, size of different mushroom is

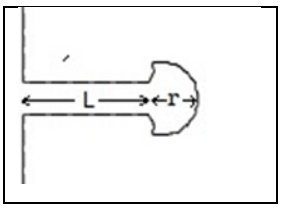

Fig (1.1): Single Protrusion

$\mathbf{A_1 = 0.87, A_2 = 3.48, A_3 = 0.87, A_4 = 1.74, A_5 = 2.61, A_6 = 1.74, A_7 = 1.74, A_8 = 2.61, A_9 = 0.87, A_{10} = 3.48, A_{11} = 1.74}$

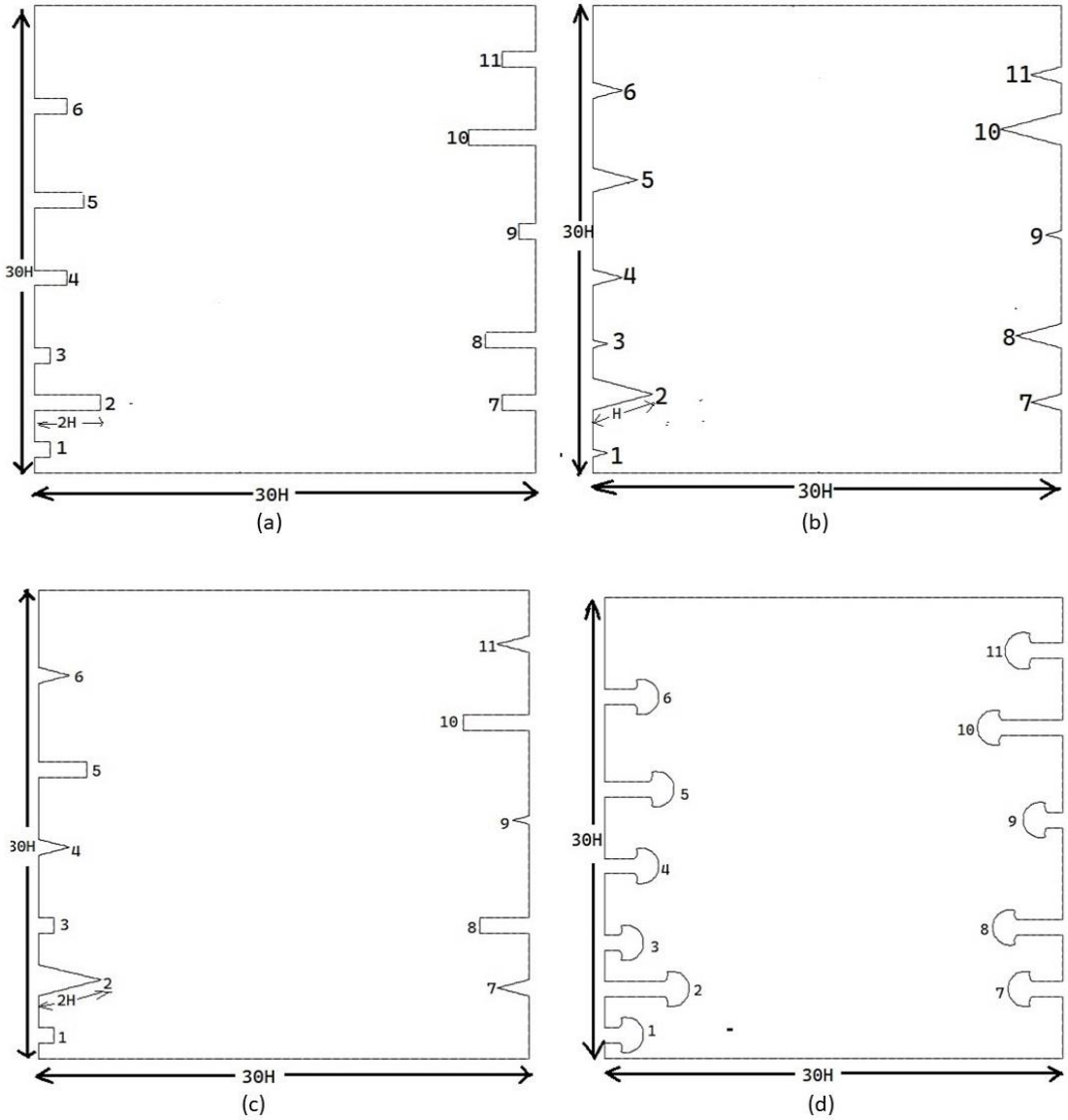

Fig (1.2):The geometry of channel with different shapes of protrusions (a) Channel with Rectangular Protrusions (b) Channel with Triangular Protrusions (c) Channel with combination of both Rectangular Protrusions and Triangular Protrusions (d) Channel with Mushroom shape of Protrusions.

2.2 Governing Equations

2.2.1 Introduction

We take into account vertical parallel channels with protrusions at the wall that have variable shaped two-dimensional, incompressible, and laminar flows. The Navier-Stokes equations and the energy equation are assumed to govern the mixed convection in a vertical channel. The fluid flow is Newtonian and all the physical properties except the density are constant but density will change and relate to the buoyance factors in the momentum equations.

To account for possible transitions to unsteady flows, the governing equations are stated in transient form.

2.2.2 Dimensional form governing equation

Conservation of mass:

$$\frac{\partial u}{\partial x} + \frac{\partial v}{\partial y} = 0$$

Conservation of momentum:

x – Momentum:

$$\frac{\partial u}{\partial \tau} + u\frac{\partial u}{\partial x} + v\frac{\partial u}{\partial y} = -\frac{1}{\rho}\frac{\partial P}{\partial x} + \mu\left(\frac{\partial^2 u}{\partial x^2} + \frac{\partial^2 u}{\partial y^2}\right)$$

y – Momentum:

$$\frac{\partial v}{\partial \tau} + u\frac{\partial v}{\partial x} + v\frac{\partial v}{\partial y} = -\frac{1}{\rho}\frac{\partial P}{\partial y} + \mu\left(\frac{\partial^2 v}{\partial x^2} + \frac{\partial^2 v}{\partial y^2}\right) + g\beta(T - T_O)$$

Conservation of energy:

$$\frac{\partial T}{\partial \tau} + u\frac{\partial T}{\partial x} + v\frac{\partial T}{\partial y} = \frac{1}{\alpha}\left(\frac{\partial^2 T}{\partial x^2} + \frac{\partial^2 T}{\partial y^2}\right)$$

2.2.3 Boussinesq approximation:

A common method for solving non-isothermal flow was the Boussinesq approximation. When density variations are small, the approximation is accurate because the nonlinearity of problem is reduced. It is assumed that differences in density have no effect on the flow field other than to cause buoyant forces.

According to the Boussinesq approximation, the density variation is only essential in the buoyancy term.

$$\rho = \rho_0[1 - \beta(T - T_0)]$$

2.2.4 Dimensionless form governing equation:

In this section, the momentum balance equation and the energy balance equation are written in a dimensionless form. The thermal conductivity, the thermal diffusivity, the dynamic viscosity and the thermal expansion coefficient are considered as constant. Moreover, the Boussinesq approximation and the equation of state are assumed to hold.

We introduce the following set of dimensionless quantities

$x^* = \frac{x}{D}$, $y^* = \frac{y}{D}$, $u^* = \frac{u}{u_\infty}$, $v^* = \frac{v}{u_\infty}$, p = $\frac{P}{\rho u_\infty^2}$, t = $\frac{u_\infty \tau}{D}$, $\theta = \frac{T - T_w}{T_\infty - T_w}$

The dimensionless governing equations are as follows:

$$\frac{\partial u^*}{\partial x^*} + \frac{\partial v^*}{\partial y^*} = 0$$

$$\frac{\partial u^*}{\partial t} + u^* \frac{\partial u^*}{\partial x^*} + v^* \frac{\partial u^*}{\partial y^*} = -\frac{\partial p}{\partial x^*} + \frac{1}{Re}\left(\frac{\partial^2 u^*}{\partial x^{*2}} + \frac{\partial^2 u^*}{\partial y^{*2}}\right)$$

$$\frac{\partial v^*}{\partial t} + u^* \frac{\partial v^*}{\partial x^*} + v^* \frac{\partial v^*}{\partial y^*} = -\frac{\partial p}{\partial y^*} + \frac{1}{Re}\left(\frac{\partial^2 v^*}{\partial x^{*2}} + \frac{\partial^2 v^*}{\partial y^{*2}}\right) + \text{Ri}\ \theta$$

$$\frac{\partial \theta}{\partial t} + u^* \frac{\partial \theta}{\partial x^*} + v^* \frac{\partial \theta}{\partial y^*} = \frac{1}{Re\ Pr}\left(\frac{\partial^2 \theta}{\partial x^{*2}} + \frac{\partial^2 \theta}{\partial y^{*2}}\right)$$

2.3 Grid Generation:

One of the important steps in carrying out an effective simulation using FEA is meshing. A high-quality mesh produces more accurate results. A poor mesh can result in convergence difficulties and it may produce inaccurate results and false conclusions. A mesh is composed of components that have nodes in them that represent the geometry's shape. Meshing is the process of transforming irregular shapes into "elements", which are more recognizable volumes.

For a simple geometry, at lower element counts, triangular elements typically produce more accurate results. The best option may be rectangular elements if the geometry is complex. In this investigation, the all geometries has been meshed with triangular elements.

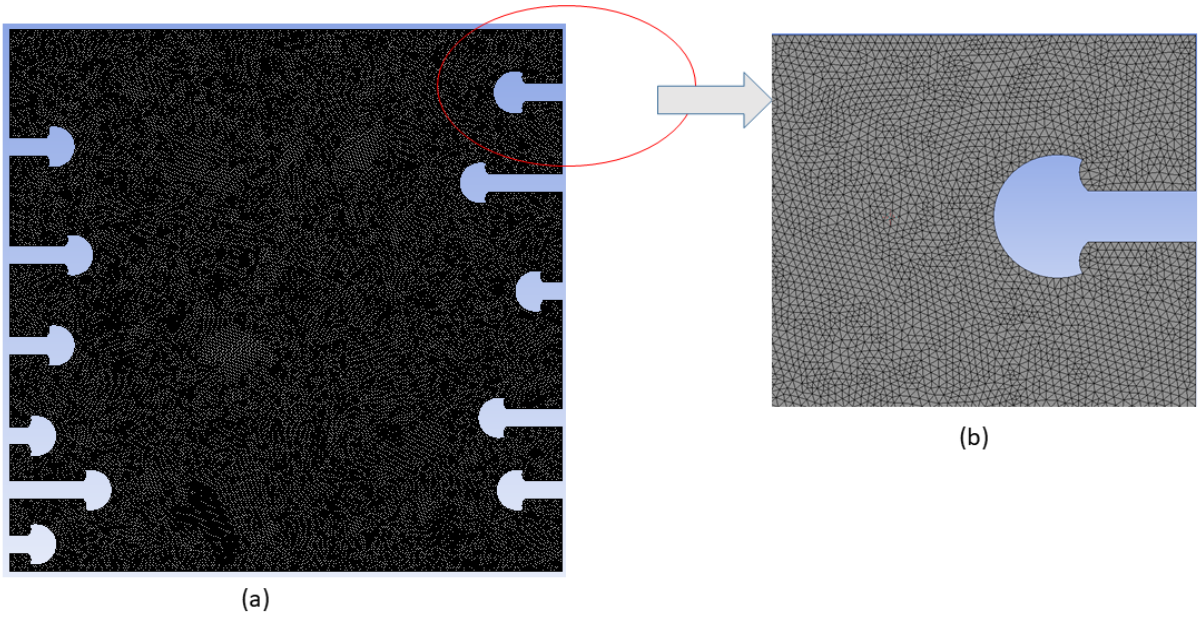

Fig (2): (a) Grid used for computation (Elements = 89537), (b) A closer view of the grid around the protrusions.

2.4 Boundary and initial conditions:

As per the boundary conditions, constant velocity and temperature at ambient condition imposed at the inlet, and at the outlet atmospheric pressure boundary condition is specified. At the walls of vertical channel and for different protrusions present at walls, no slip condition with constant temperature is specified. The initial and boundary conditions, in dimensionless form, used for the components of velocity and for the temperature are:

At inlet; U = 0, V = 1 and $\theta = 0$

At exit; P = 0 Pa

At walls and Protrusions; U = 0, V= 0, θ=1

Chapter 3

Model Implementation

3.1 Solution Methodology

In a commercial CFD software FLUENT 2021 R2, the governing equations and the aforementioned boundary conditions are solved using a pressure-based segregated solver. The finite volume method (FVM) was used to spatially discretize the conservation equations to second order on a structured grid with co-localization of variables occurred at the centre of the mesh. The fundamental principle of the FVM is to divide flow domain into control volumes, and then governing equations are integrated across each finite control volume (each mesh cell). This leads to a set of algebraic equations with the unknown field variable and a sparse coefficient matrix. Each algebraic equation will relate the value at the cell centre to the neighbour to it. In order to solve this linear system for scalar equations, ANSYS- FLUENT combines point implicit (Gauss-Seidel) linear equation solver with an algebraic multigrid (AMG) technique. After being computed, the field variables are stored in the centroids of the each finite volume cells and hence the name ’cell-centred’ FVM.

3.1.1 Pressure-Based Solver

The algorithm used by the pressure-based solver is a member of a broad class of techniques known as the projection method. In this method, a pressure (or pressure correction) equation is solved to satisfy the constraint of mass conservation (continuity) of the velocity field. The pressure equation is derived from the continuity and the momentum equations in such a way that the velocity field, corrected by the pressure, satisfies the continuity. Since the governing equations are nonlinear and coupled to one another, the solution process involves iterations wherein the entire set of governing equations is solved repeatedly until the solution converges. In ANSYS FLUENT, there are two pressure-based solution algorithms available, a coupled algorithm and a segregated algorithm.

3.1.2 The Pressure-Based Segregated Algorithm

The governing equations are solved separately from one another in the solution algorithm used by the pressure-based solver. Due to the non-linear and coupled governing equations, an iterative solution loop is required in order to get a converged numerical solution.

In the segregated algorithm, the individual governing equations for the solution variables such as $u, v, w, p, T, k\ etc$. are solved one after another. Each governing equation, while being solved, is "decoupled" or "segregated" from other equations, hence its name. The discretized equations only need to be stored in the memory one at a time, making the separated algorithm memory-efficient. Since the equations are solved in a decoupled way, the convergence of the solution happens relatively slowly.

With the segregated algorithm, each iteration consists following of the steps as given in fig (3) and outlined below:

1) Based on the current value of pressure and temperature, fluid characteristics (e.g. density, viscosity, specific heat) are updated. If the calculation has just started, the fluid characteristics will be updated based on the initial values of x and y velocities, pressure.
2) Using the recently updated values of velocity and pressure, solve the momentum equations, one after another.
3) Use most recently updated value of velocity field and the mass-flux to solve the pressure correction equation.
4) Using the pressure correction from Step 3, correct the velocity field, face mass fluxes, and pressure.
5) Solve the equations for additional scalars.
6) The source term should be updated to reflect the interactions between the various phases.
7) Check for the convergence of the equations.

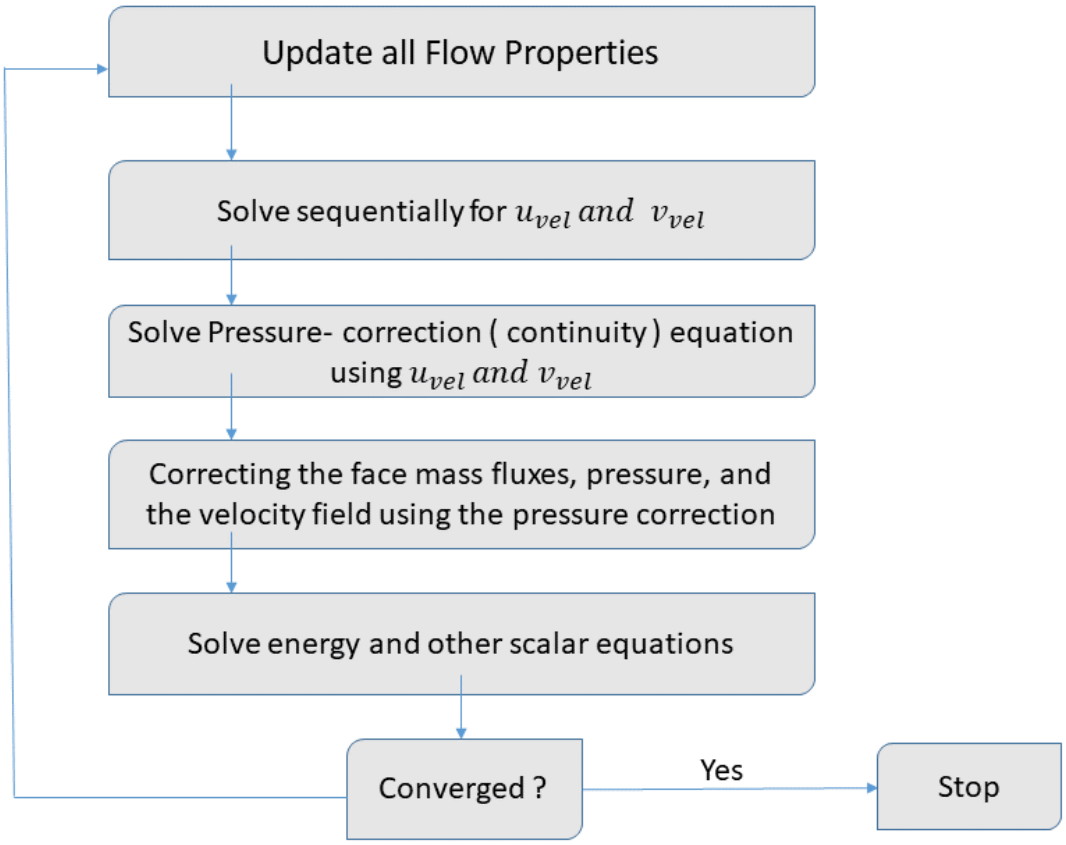

Figure (3.1): Overview of the Pressure-Based Segregated Algorithm

3.1.3 Convergence Criterion

When using an iterative solution method, a convergence and stopping criterion must be established in order to end the iteration process. The measure of convergence is a norm on the change in the solution vector between successive iterations. If the convergence has not been achieved after a fixed number of iterations, the iterative algorithm is terminated. This criterion is used to avoid wasting computation time on slowly convergent or divergent problems. In this study, convergence is considered as having been obtained when all of the following criteria are met.

Changes in the continuity is less than $1x10^{-6}$

Changes in the x - and y - velocity component are less than $1x10^{-6}$

Changes in the energy is less than $1x10^{-10}$

3.2 Mesh Independence Analysis

To evaluate the accuracy of the numerical model and make sure that the flow parameters do not change along with cell sizes, a mesh independence study has been carried out**.** The simulation setup for the mesh sensitivity test for six different mesh densities is tabulated in Table (3.2.1). The parameter chosen for independency test is the wall heat flux (q) for left wall. Figure 3.2 shows the grid independence study clearly indicating mesh independence at a mesh size of 15 mm with a difference in Wall heat flux q within 1%.

Table (3.2.1): Mesh statistics for grid divergence test

Mesh Number	Minimum Mesh Size (mm)	Cell Count	q (Left wall) [W/m^2K]	% difference
1	0.16	35121	172.143	0.021
2	0.15	40029	172.107	0.375
3	0.14	45563	172.755	0.395
4	0.13	53708	173.441	0.177
5	0.12	62516	173.749	0.130
6	0.11	73765	173.976	

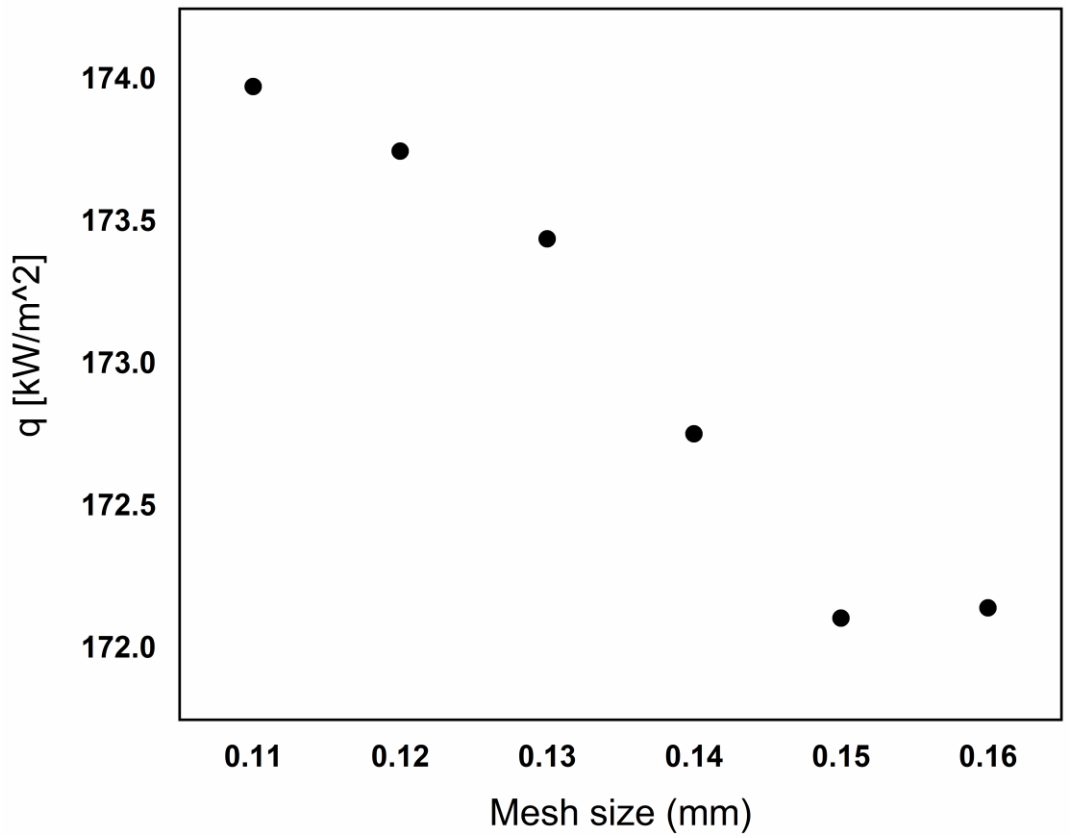

Fig (3.2): Results from grid convergence study showing the dependence of the wall heat flux (q) on the number of mesh elements.

Chapter 4

Model Validation

To validate the current computational method, the computational results of some selected cases were compared with the experimental results of by Habchi and Acharya (1986)[14] . They measured air velocity profiles caused by laminar mixed convection in a vertical channel with a partly rectangular obstruction on one channel wall. The blocked wall is supposed to be heated, whereas the other wall is assumed to be adiabatic. It is seen that the simulation result agrees well with the literature data within a maximum deviation of 5 %. Fig (4.1) compares the temperature distribution across the asymmetrically heated channel with the experimental and numerical results of Habchi and Acharya (1986)[14]. Again, a good agreement is seen with the present work. Finally, in Figure (4.2), compares the velocity distribution across the asymmetrically heated channel with the experimental and numerical results. Again, the model predictions from this investigation are shown to agree satisfactorily with the data given in the literature.

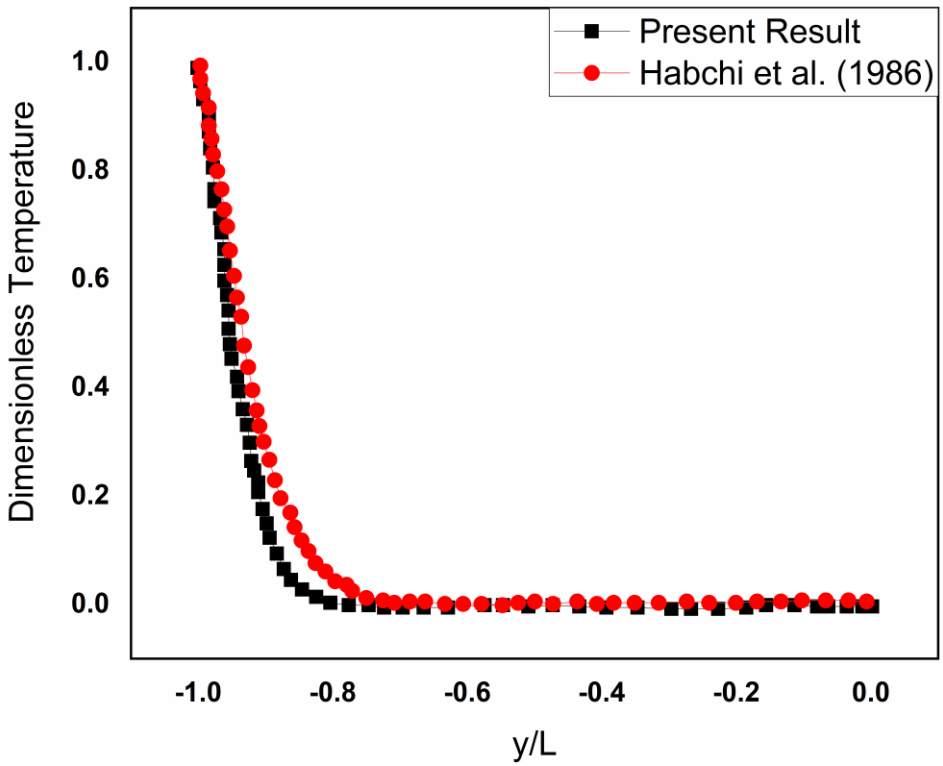

Figure (4.1): Comparison of the temperature distribution across the asymmetrically heated channel with the experimental and numerical results of Habchi $et\ al.$ (1986)[14] at y/L = 0.77.

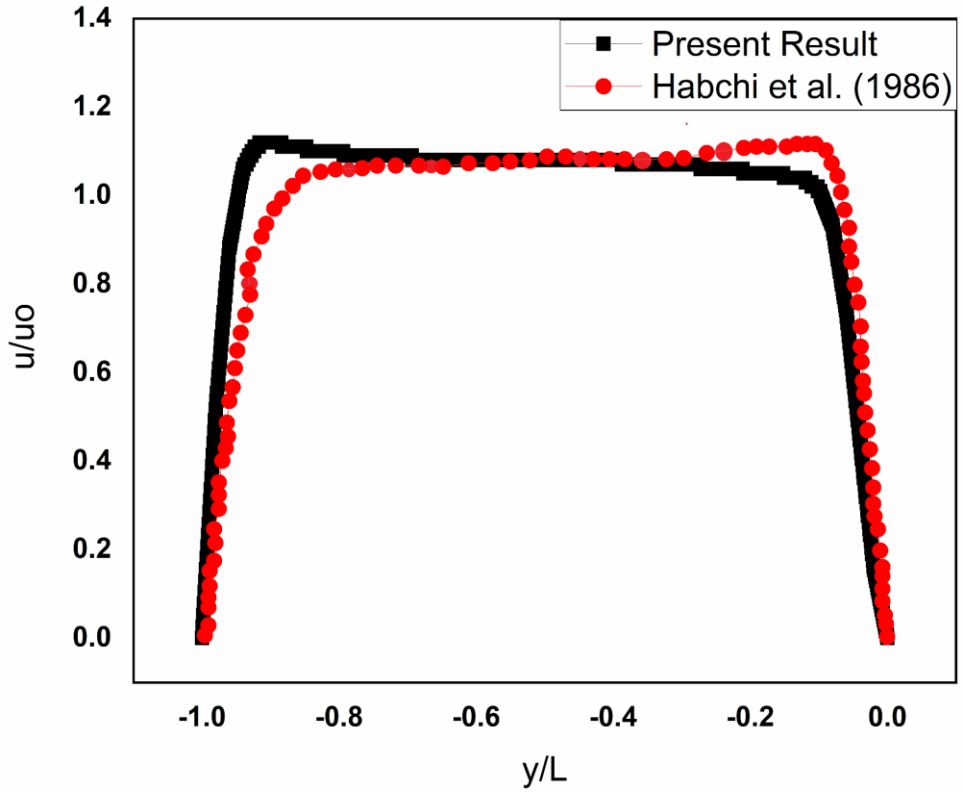

Fig (4.2): Comparison of the velocity distribution across the asymmetrically heated channel with the experimental and numerical results of Habchi $et\ al.$ (1986)[14] at y/L = 0.77.

Chapter 5

Results & Discussions

In this chapter, for the laminar regime, the heat transfer and fluid flow properties of mixed convection in a Vertical Parallel-plate channel with different shapes of protrusions are investigated.

5.1 Variation of Wall Heat Flux along the vertical wall:

The wall heat flux data in all of the figures exhibit a common pattern. In general, heat transfer rate begin high at the leading edge of every protrusions and then sharply decline to a very low value at the junction and walls of the protrusions. Also, heat transfer rate fluctuations along the wall profile co-ordinate are periodic in nature, with the frequency equal to the projection of the protrusions on the wall in vertical direction. There are two distinct thermal behaviour zones exist in the diagram, one is the protrusions and other is region between two protrusions (i.e. portion of wall between two protrusions). First, we give our attention to the thermal performance along the protrusions. The distribution of wall heat flux along the horizontal surfaces of protrusions (in rectangular protrusions) and inclined surface (in triangular protrusions) indicates that the main flow tends to skip the projecting parts which behave as impediments to induced convection currents through the channel. But, in case of vertical sides of protrusions (in rectangular protrusions) and curved surface (in mushroom protrusions) and especially at their leading edges, effective heat transfer conditions exist because they are washed by relatively cool air flow through the channel. For the reasons mentioned previously, wall heat flux distributions along the regions between two protrusions are characterised by very low values close to the protrusions. On the other hand, the gap between the protrusions is large enough for the main flow to wash the inter- protrusions surfaces before being redirected by the next protrusions downstream. This explains why the heat transfer peaks roughly between the midpoints of region between two protrusions. It is already observed that distributions of heat transfer rate between subsequent couples of protrusions are similar. But, when we compare values of heat transfer at places separated by an elevation equal to the projection of the protrusions on the wall, it gradually decline from bottom to top of the vertical channel according to the size of the protrusions. This is due to the developing thermal field

and here, assumed wall heat flux being based on the temperature difference between the heated vertical wall and the inlet (not bulk) fluid.

For Left Wall having six protrusions

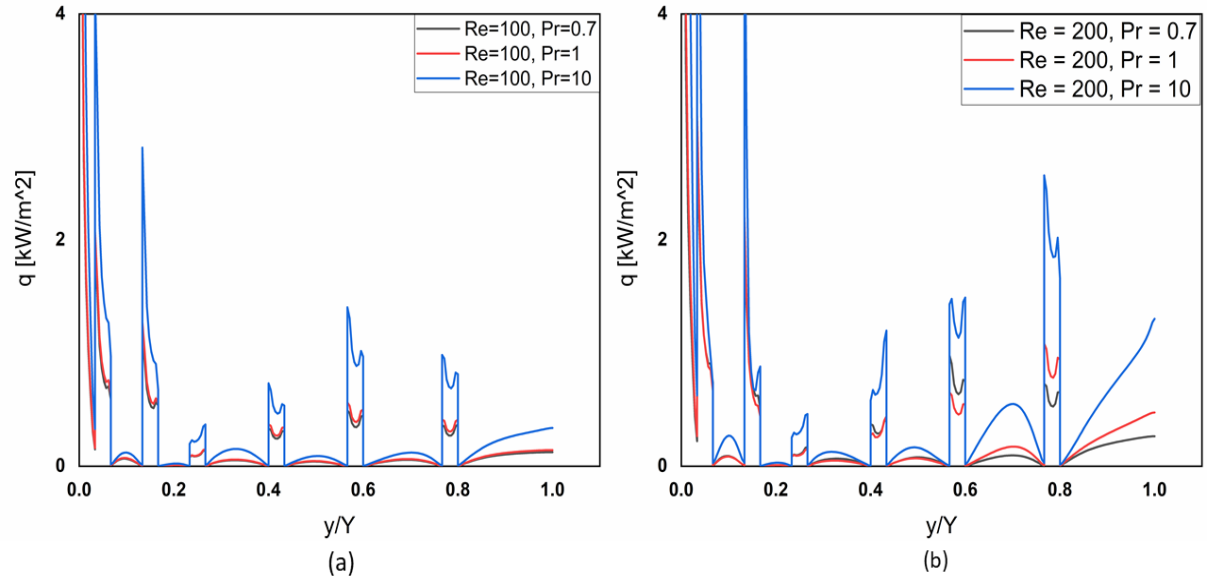

Fig (5.1.1): The variation of wall heat flux with Rectangular Shape of protrusions (Left Wall) for Re=100 (a) and Re=200 (b) for various Prandtl Number.

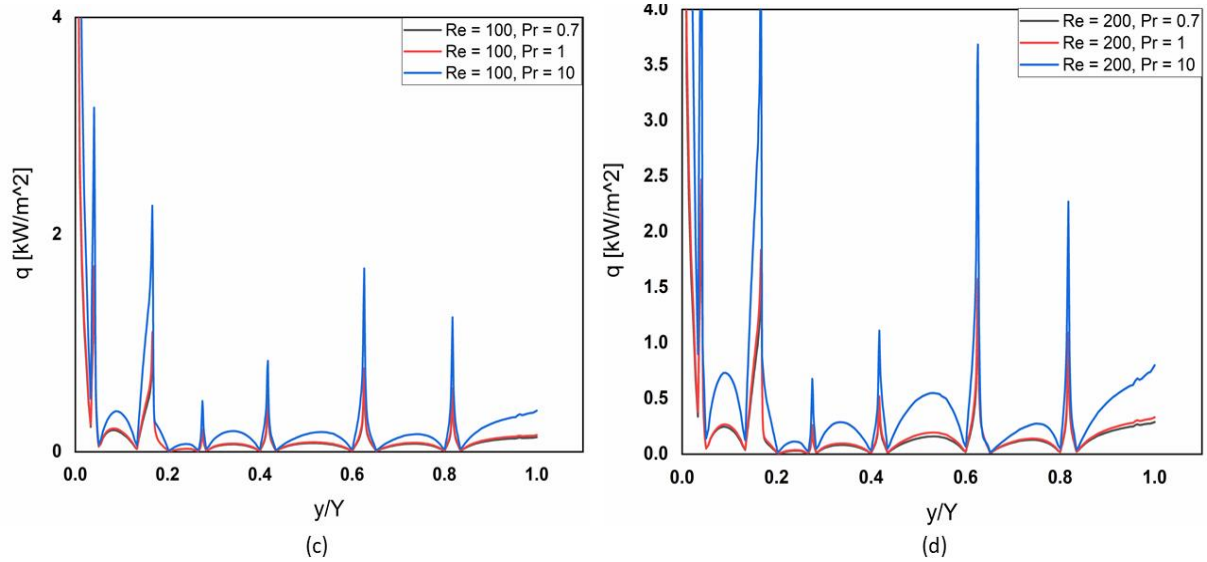

Fig (5.1.2): The variation of wall heat flux with Triangular Shape (Left Wall) of protrusions for Re=100 (c) and Re=200 (d) for various Prandtl Number.

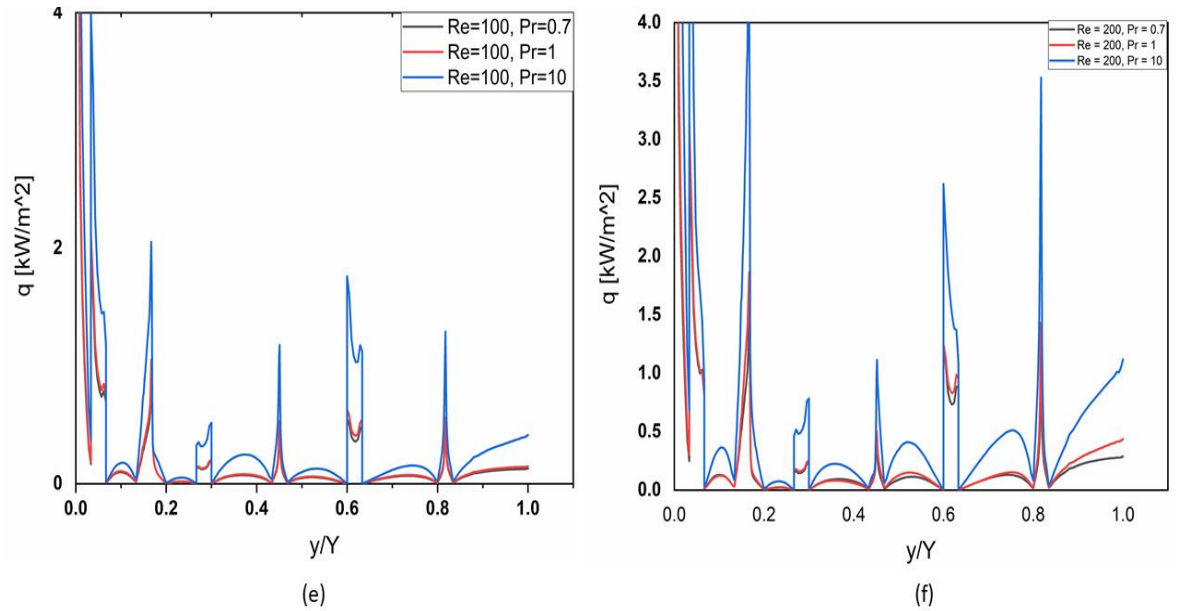

Fig (5.1.3): The variation of wall heat flux with combination of both Rectangular and Triangular Shape of protrusions (Left Wall) for Re=100 (e) and Re=200 (f) for various Prandtl Number.

In fig (5.1.3), we clearly obsever that for first quarter from inlet, the wall heat flux for combination of Rectangular and Triangular Shape of protrusions lies between wall heat flux of Rectangular Shape of protrusions and Triangular Shape of protrusions because here less surface area available for heat transfer and blockage of fluid is less than Rectangular Shape of protrusions. So, fluid easily washed the surface of the protrusions.

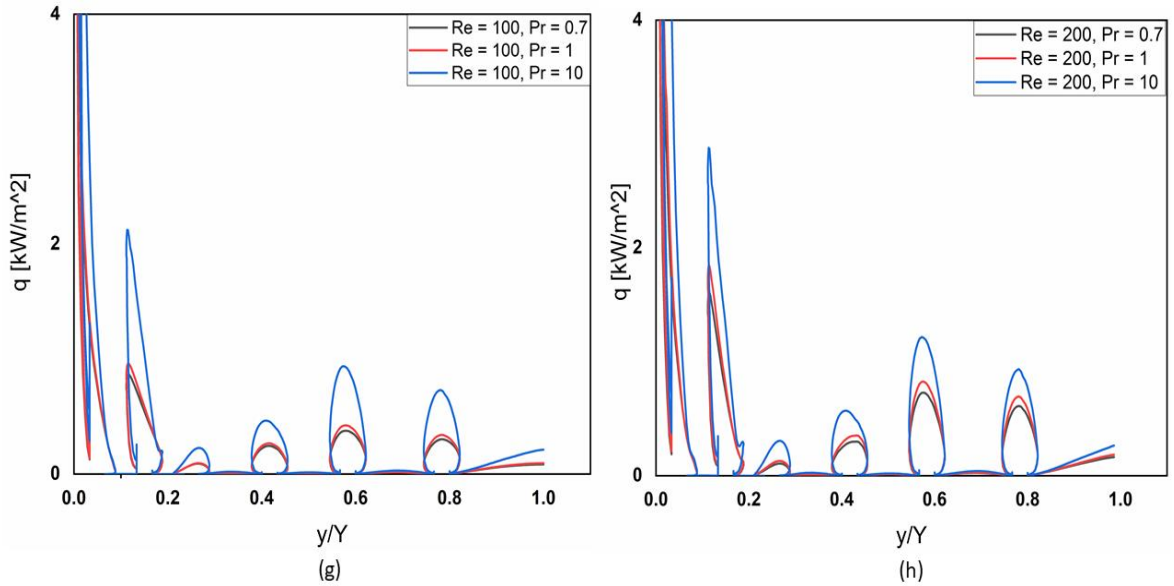

Fig (5.1.4): The variation of wall heat flux with Mushroom Shape (Left Wall) of protrusions for (g) Re=100 and (h) Re=200 for various Prandtl Number.

For Mushroom Shape of protrusions, in fig (5.1.4), we clearly observe that overall wall heat flux is more than other shape of protrusions because here, more surface area available for heat transfer and blockage of fluid is also more due to curve shape of the protrusions. Also, from above graph we say that area of heat transfer for same value of Reynold's Number and Prandtl Number is more for Mushroom shape of protrusions than other shape.

For Right Wall having five protrusions

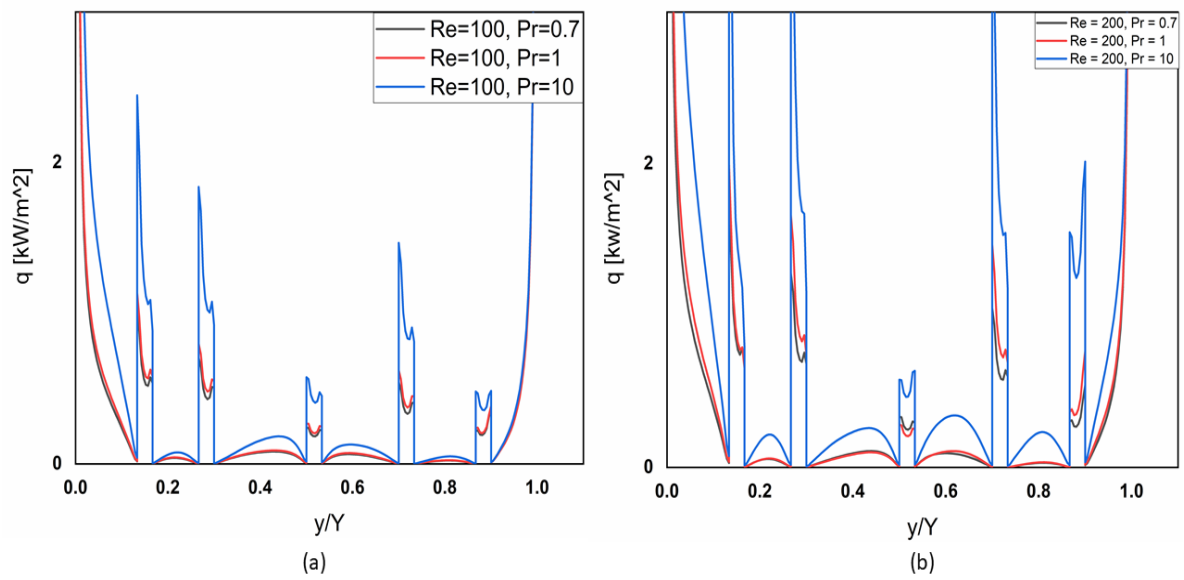

Fig (5.1.5): The variation of wall heat flux with Rectangular Shape (Right Wall) of protrusions for Re=100 (a) and Re=200 (b) for various Prandtl Number.

For the right wall, we clearly observe in fig (5.1.5) that less wall heat flux for first quarter from inlet because there is less protrusions present as compared to left side of wall. So, surface area available for heat transfer is less and blockage of fluid is also less. Fluid flowing through protrusions of right wall, washed the protrusions surface easily.

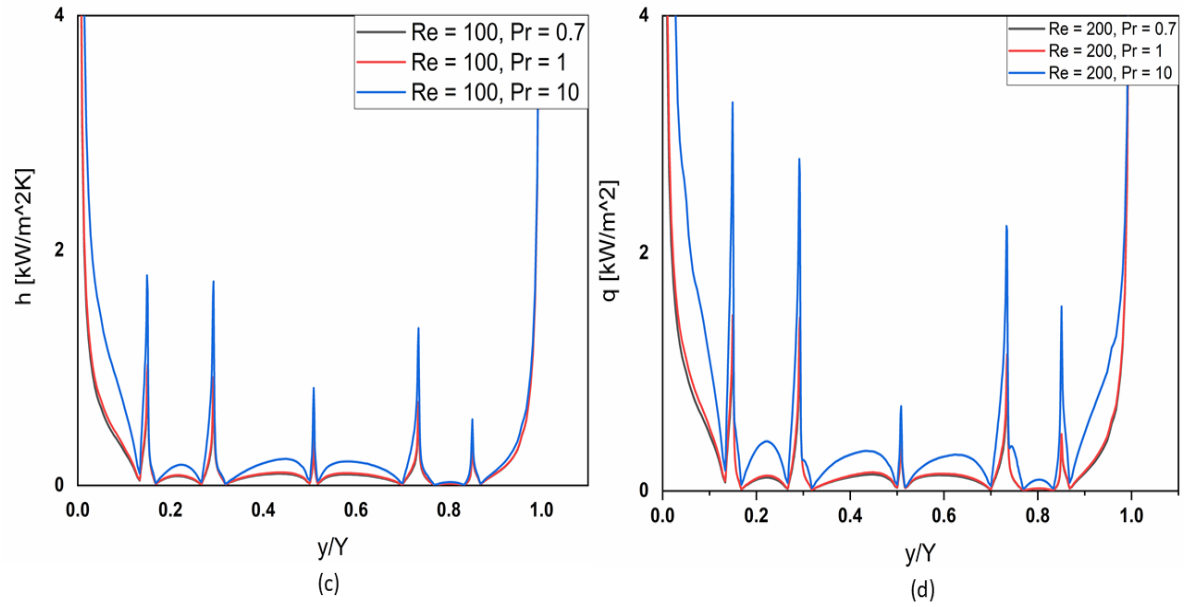

Fig (5.1.6): The variation of wall heat flux with Triangular Shape (Right Wall) of protrusions for Re=100 (c) and Re=200 (d) for various Prandtl Number.

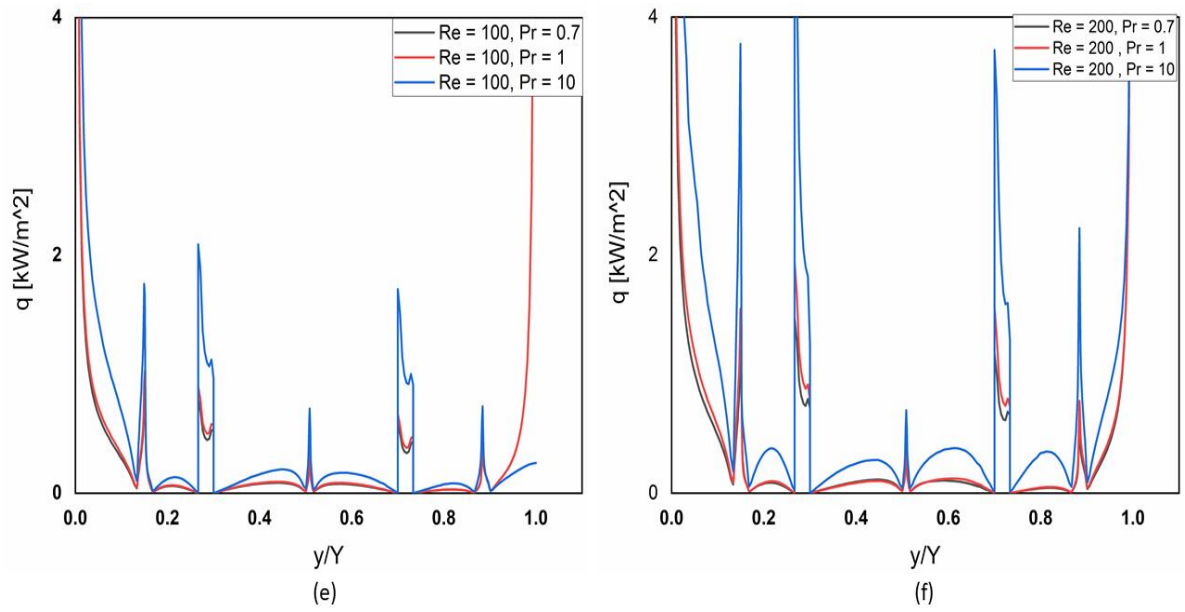

Fig (5.1.7): The variation of wall heat flux with combination of both Rectangular and Triangular Shape of protrusions (Right Wall) for Re=100 (e) and Re=200 (f) for various Prandtl Number.

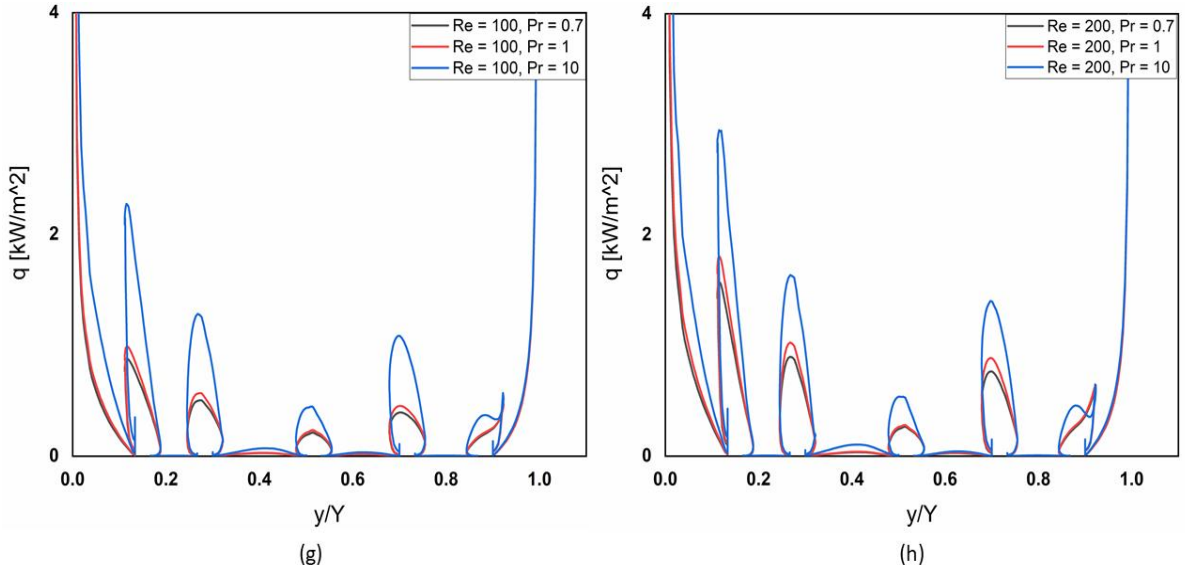

Fig (5.1.8): The variation of wall heat flux with Mushroom Shape (Right Wall) of protrusions for Re=100 (g) and Re=200 (h) for various Prandtl Number.

For right wall, there are five protrusions present at wall so less surface area available for heat transfer. Also, gap between two protrusions are more so, there is no much blockage of fluid

happen here as compare to left wall. Due to this reason, less heat transfer takes place through left wall for respective protrusions and the gap between the protrusions is large enough for the main flow to wash the inter- protrusions surfaces before being redirected by the next protrusions downstream.

So in fig (5.1.5) to fig (5.1.8), we clearly observe that for the increase in Re and Pr, we found similar trend for wall heat flux as we have seen in case of left wall. Here, also maximum wall heat flux for Mushroom shape of protrusions because it has more area available for heat transfer. As Re and Pr increases, wall heat flux also increases but increment is less than protrusions of left wall.

5.1.1 Effect of dimensionless parameter on vertical wall

5.1.1.1 Effect of Prandtl Number

In fig (5.1.1) to (5.1.8), we clearly observer that for Re = 100 and Re = 200 in case of a particular shape of protrusions as Pr increases from 0.7 to 10, wall heat flux also increases. We know, Prandtl number is the ratio of momentum diffusivity to thermal diffusivity. An increase in the Prandtl number reduces the thermal boundary layer thickness. The Prandtl number (Pr) of a fluid gives the relative importance of the momentum boundary layer to the thermal boundary layer in heat transfer problems. When Pr is small, heat diffuses fast in comparison to velocity (momentum), hence the thickness of the thermal boundary layer for liquid metals is significantly greater than that of the momentum boundary layer. A high Pr value indicates that heat transfer by fluid momentum is preferable to thermal diffusion. In other words, a high Pr value indicates that heat transfer is more likely to occur by fluid momentum rather than fluid conduction. Also, we can see there is same trend of variation of wall heat flux for Re = 200 with different value of Pr.

5.1.1.2 Effect of Reynold's Number

In fig (5.1.1) to fig (5.1.8), we can observe that as Re increases from 100 to 200, value of wall heat flux also increase. At low Re, the buoyancy effect is greater than the forced convection effect and also, the thermal boundary layer thickens and the temperature gradient shifts more toward the normal flow direction. In other words, the temperature gradient is greater at high Reynolds numbers than at low Reynolds numbers. As, Re increases, it also increase the turbulence in fluid flow. The formation of turbulence is largely influenced by the initial disturbance in the flow, and the presence of turbulence enhances heat transfer. As the fluid's velocity increases, it will ultimately reach a point where it will generate turbulence eddies where the boundary layer breaks away from the wall and mixes with the bulk of the fluid further away from the channel wall. So, the thickness of the boundary layer deceases with increase in Re and it results in increases of heat transfer from the channel wall and protrusions. As a result, the rate of heat transfer is greater at high Re than at low Re.

5.2 Velocity and Temperature contour

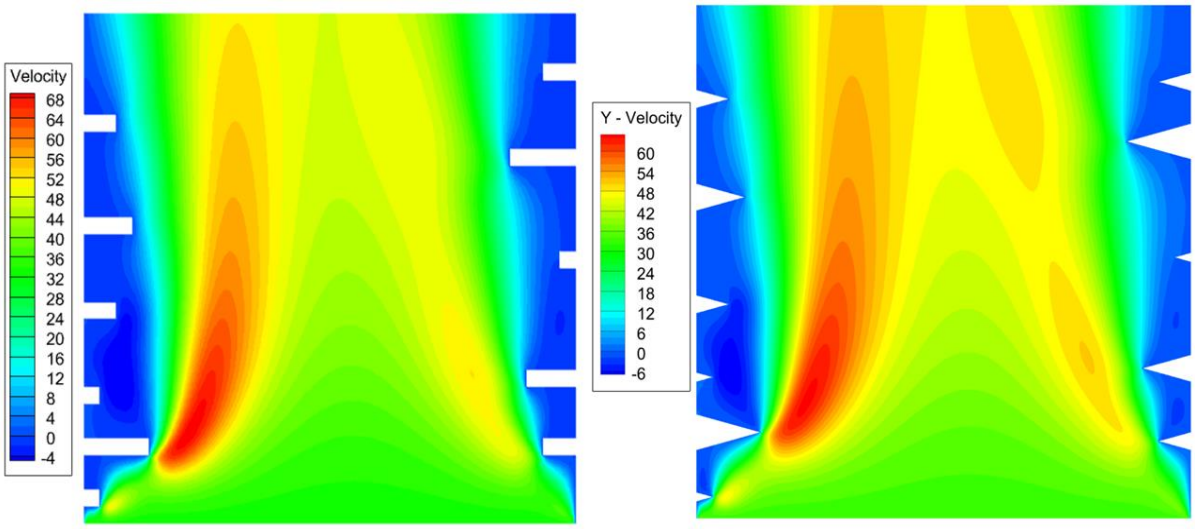

(a) (b)

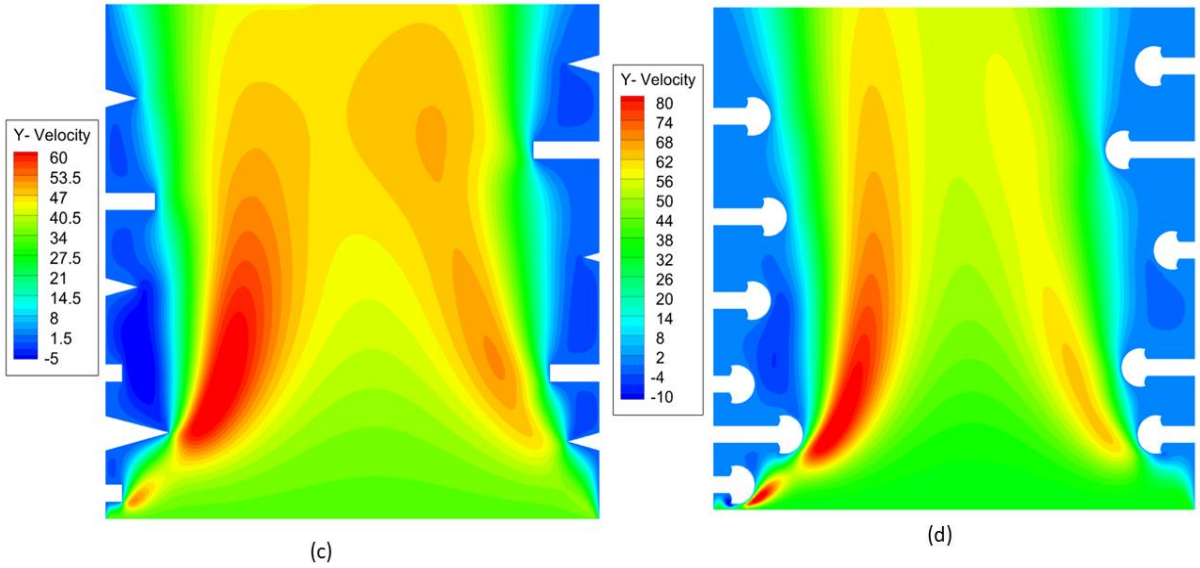

Fig (5.2.1): The velocity contour for (a) Rectangular protrusion (b) Triangular protrusion (c) combination of both (d) Mushroom protrusion

For a particular shape of protrusions, velocity reduction near the wall due to buoyancy opposes the flow can be seen from figure (5.2.1). As buoyancy increases the temperature and velocity near the heated wall decrease. Hence, the temperature gradients fall down with respect to increase in buoyancy force in opposing flow near the wall which results in reduction in wall heat flux near the wall.

The figures (5.2.1) also show that near right wall where protrusions spacing is more, increasing the protrusions spacing decreases the flow speed through the channels. The formation of boundary layers on the sides of protrusions begins to narrow the channel, reducing the flow speed across it.

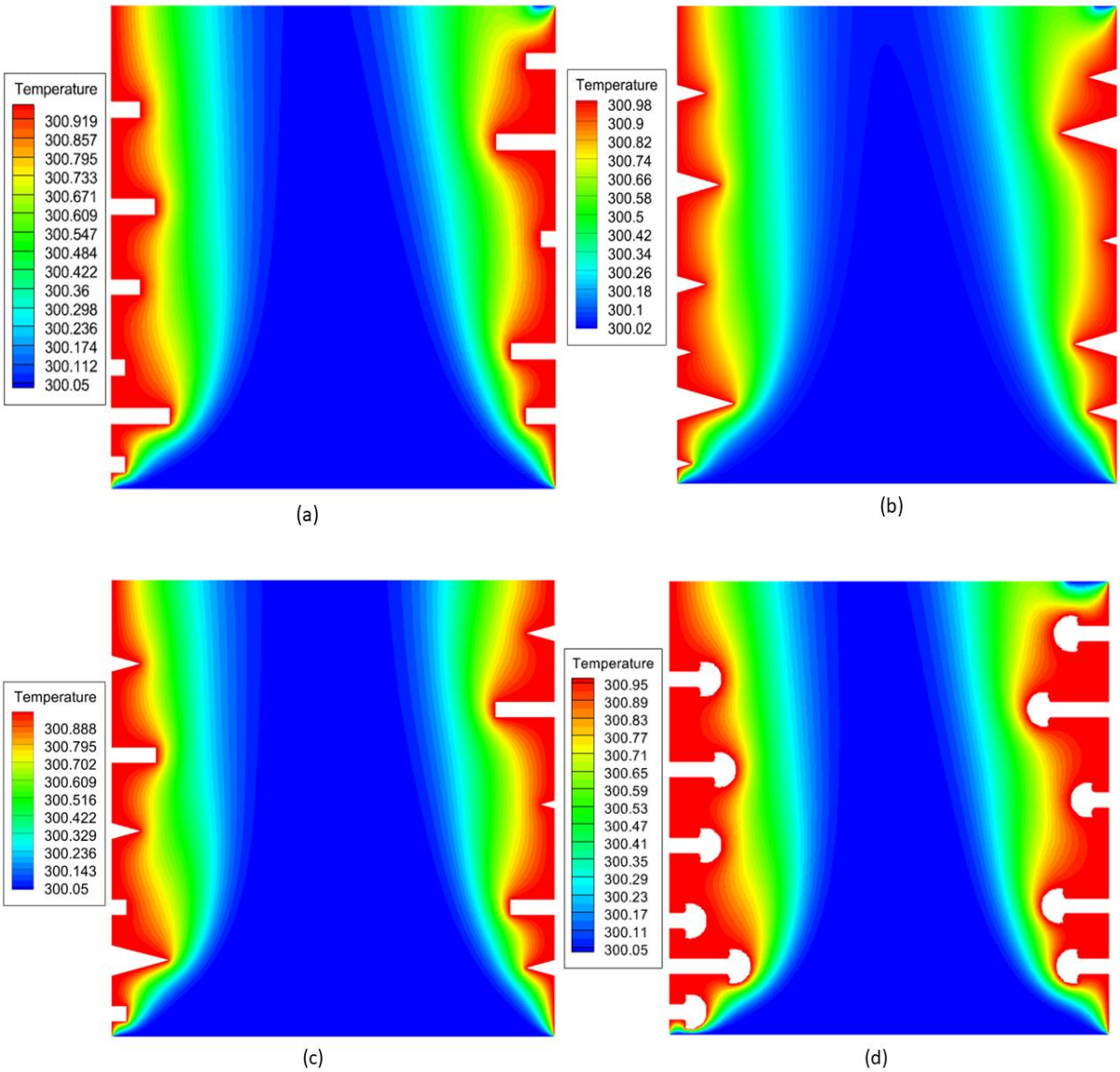

Fig (5.2.2): Temperature contour for (a) Rectangular protrusion (b) Triangular protrusion (c) combination of both (d) Mushroom protrusion

Figure (5.2.2) illustrates the temperature distribution of through vertical channel for different shapes of protrusions. The temperature gradients increases as buoyancy increases, resulting in an increase in velocity near the wall and temperature decreases.

5.3 Streamlines and isotherms:

In figures (5.3.1) to (5.3.3) the result of streamlines and isotherms are plotted. It is observed that recirculating flows occur between and near the protrusions and the flow pattern and size of recirculation around each protrusion is also depend upon shape of the protrusions. While the recirculation intensity between the first two protrusions is rather weak, but as we go towards the outlet of the channel recirculation intensity between the other protrusions rises as the momentum of hot air increases.

Corresponding to these flow patterns, the isothermal lines are densely distributed near the protrusion. This indicates that the heat transfer rates are higher in these regions. The local heat transfer rate at the leading edge of each protrusion is greater than that near the trailing edge, and those on vertical surfaces become low due to the slow recirculating flow between and near the protrusions.

In general, the isotherm contours clearly show the dead zones immediately upstream and downstream of each protrusions, as well as the high heat transfer performance wall sections on the vertical sides of the protrusions and between the protrusions, where the thermal boundary layer is relatively thin.

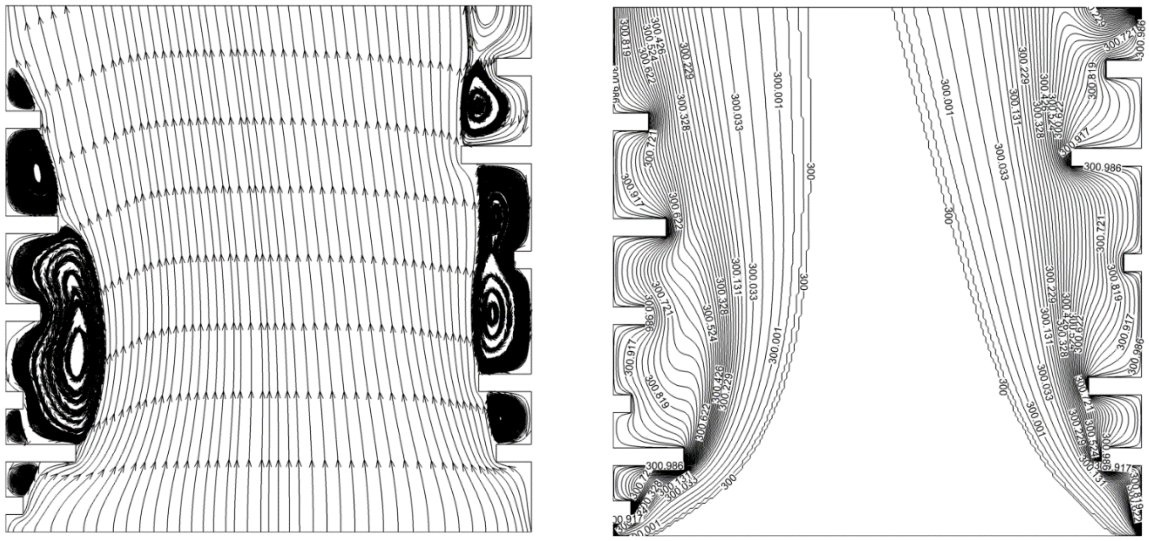

(a) (b)

Fig (5.3.1): Streamlines (a) and isotherms (b) are plotted for Rectangular Protrusion.

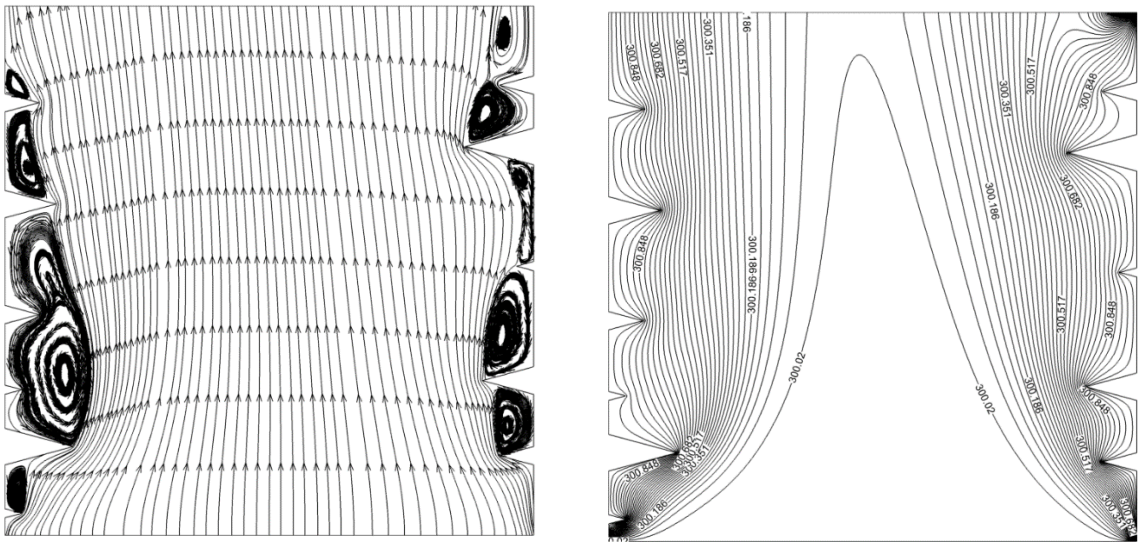

(c) (d)

Fig (5.3.2): streamlines (c) and isotherms (d) are plotted for Triangular shape of protrusion.

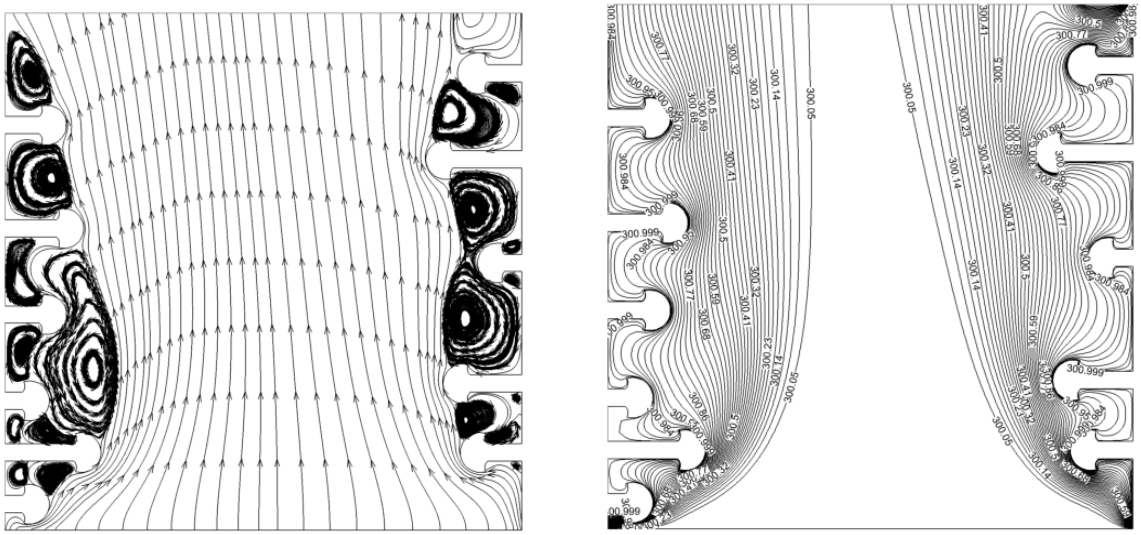

(e) (f)

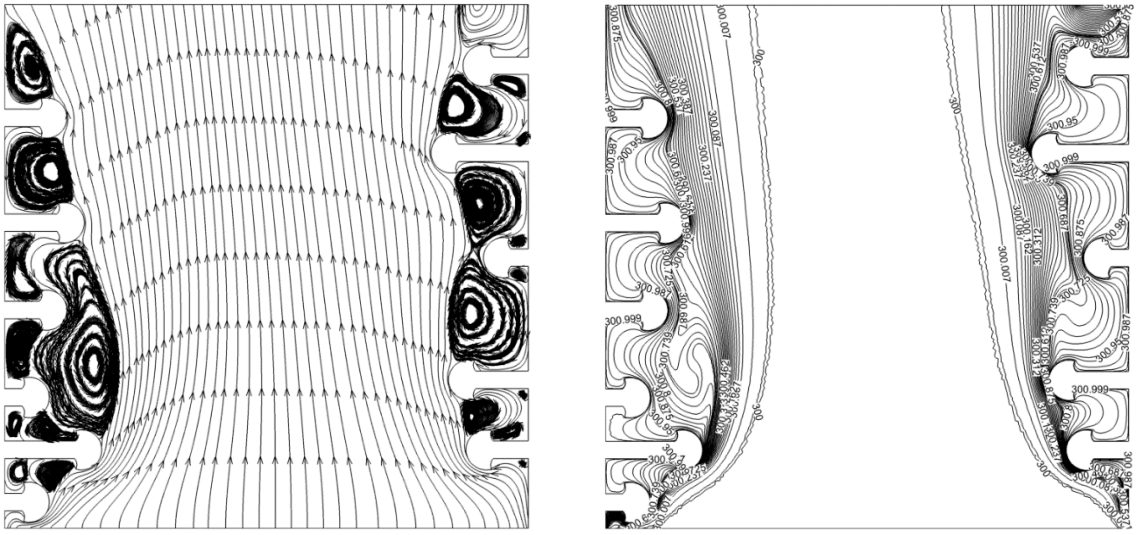

(g) (h)

Fig (5.3.3): Streamlines are plotted (e) for Re=100 and (g) for Re=200 and isotherms are plotted (f) for Re=100 and (h) for Re=200 for Mushroom Shape of Protrusions.

5.4 Variation of Temperature at a plane nearby of protrusions

Fig. (5.4.1) to fig. (5.4.3) shows the variation of the temperature at a plane nearby of protrusions with Reynolds number for various shapes of protrusions at the walls. It shows that variation of temperature decreases with increasing Re. This improves the heat transfer and is related to the flow of recirculation that occurs between the protrusions and the decrease in the thickness of the thermal barrier layer. Near left wall, plane is taken at x=6H and near right wall, plane is taken at x =24H. At a plane near of left wall, the temperature rises slowly until it reaches the first quarter of the wall, after which it rapidly rises. From the maximum, the temperature drops again sharply to some lower value, before becoming asymptotic towards the channel exit. In the first quarter, near of left wall due to less spacing between protrusions, blockage of fluid takes place so temperature in first quarter rises but after this region protrusions are small and far enough from each other so that fluid easily wash away the surface of the protrusion so temperature after first quarter decreases. It also indicates heat transfer rate decreases in this region. So, if the protrusions spacing is decreases, average temperatures of the fin arrays again increase.

But, for plane near of right wall having less number of protrusions and spacing between protrusions is more and there is not much blockage for fluid flow so in the figure (5.4.1)

to (5.4.2), we see that temperature at a plane nearby of right wall continuously rises and it reaches maximum value at outlet but in fig (5.4.3)(f) for Mushroom shape of protrusions, after peak of maximum temperature there is small decrement in temperature due to blockage of fluid by its curved part. It can be observed that when the protrusions spacing is increased the average temperatures of the protrusions arrays increase rapidly.

The protrusions in the entrance region interacts with colder air at first. Therefore, temperature of the first protrusions is lower than other, and temperatures of the protrusions gradually increase and reaches maximum then gradually decreases towards the channel exit.

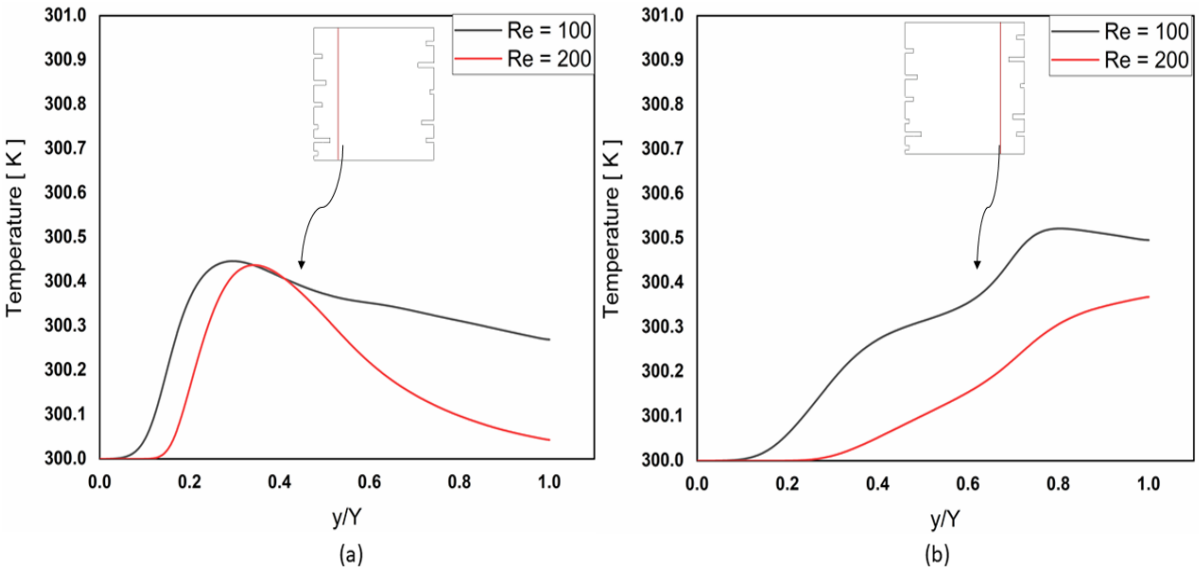

Fig (5.4.1): The variation of temperature for Rectangular Protrusions at a plane nearby (a) left wall at x = 6H and (b) right wall at x = 24H for Re =100 and 200.

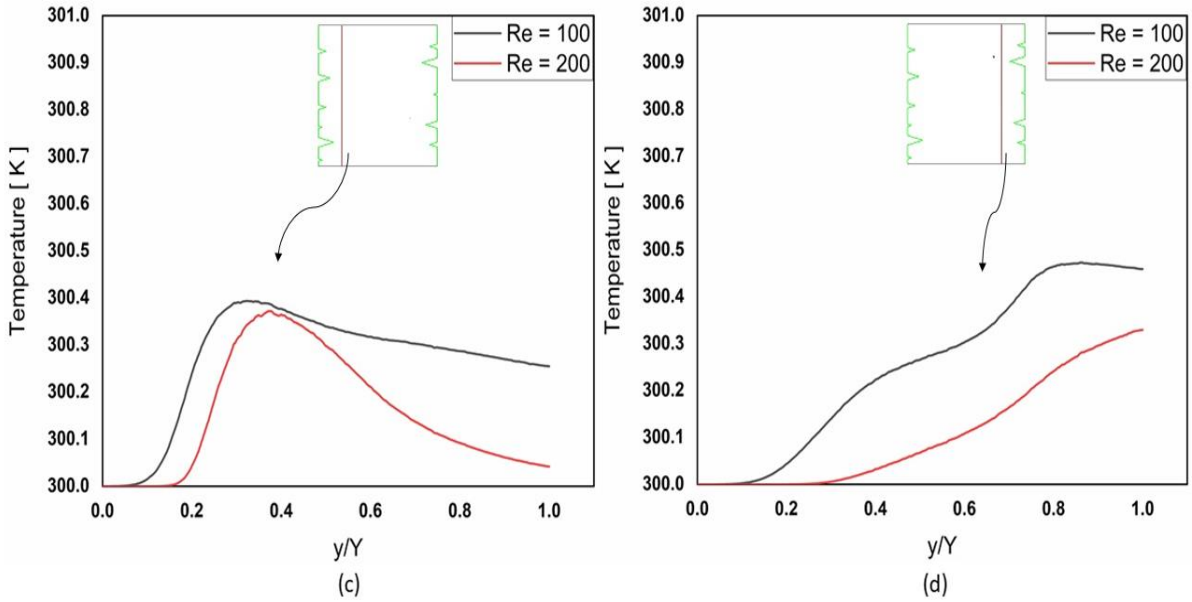

Fig (5.4.2): The variation of temperature for Triangular Protrusions at a plane nearby (a) left wall at x = 6H and (b) right wall at x = 24H for Re =100 and 200.

We clearly observe in fig (5.4.1) and fig (5.4.2) that for the first quarter of channel nearby of left wall temperature rises reaches maximum and it decreases afterward. At inlet, as shape of protrusions decreases from inlet to first quarter so wall heat flux is maximum for first protrusions and it decreases till third protrusions so, nearby of third protrusions temperature is highest which indicates wall heat flux minimum for third protrusion for a particular shape as here, temperature difference is also responsible for heat transfer. Figure also indicates that for higher Reynold's Number, temperature rise is less. As fluid velocity increases, there is more heat transfer takes place from protrusions.

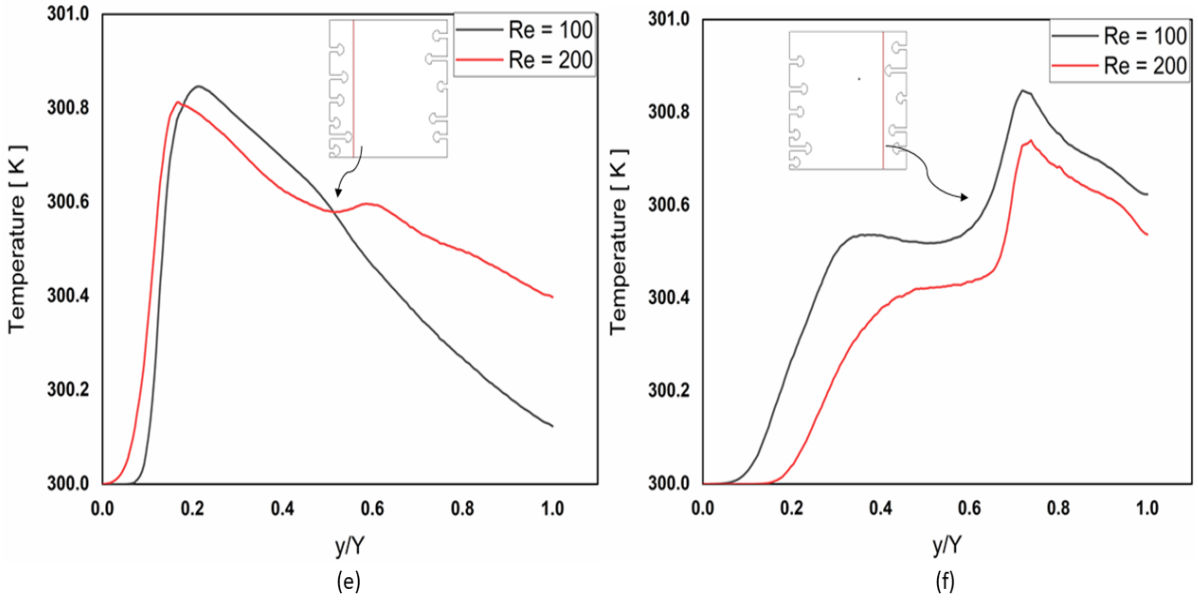

Fig (5.4.3): The variation of temperature for Mushroom Protrusions at a plane nearby (a) left wall at x = 6H and (b) right wall at x = 24H for Re =100 and 200.

5.5 Performance comparison of Mushroom Shape of protrusions with other

There is a sudden enlargement in the case of all protrusions due to random size and random space between protrusions. It creates a recirculation zone. As a result, the backflow produced reduces the induced buoyant flow and causes the wall heat flux to decrease along the vertical direction but in fig (5.3.3) (e) & (g), we clearly observe that for Mushroom shape of protrusions at left wall , due to sudden blockage, it crates large recirculation zone at quarter portion of vertical channel than other shape of protrusions so, value of h is highest at quarter portion because thermal boundary layer becomes thinner along the heated wall, and convective heat transfer from the heat sources to the air gradually increases up to this portion. But, in case of other protrusions like rectangular and triangular, there is less blockage of air flowing through channel as compared to Mushroom shape of protrusions so flowing air washed the heated surface and there is less effect of recirculation on wall heat flux and heat transfer co-efficient as here, these parameter also depend upon the bulk fluid.

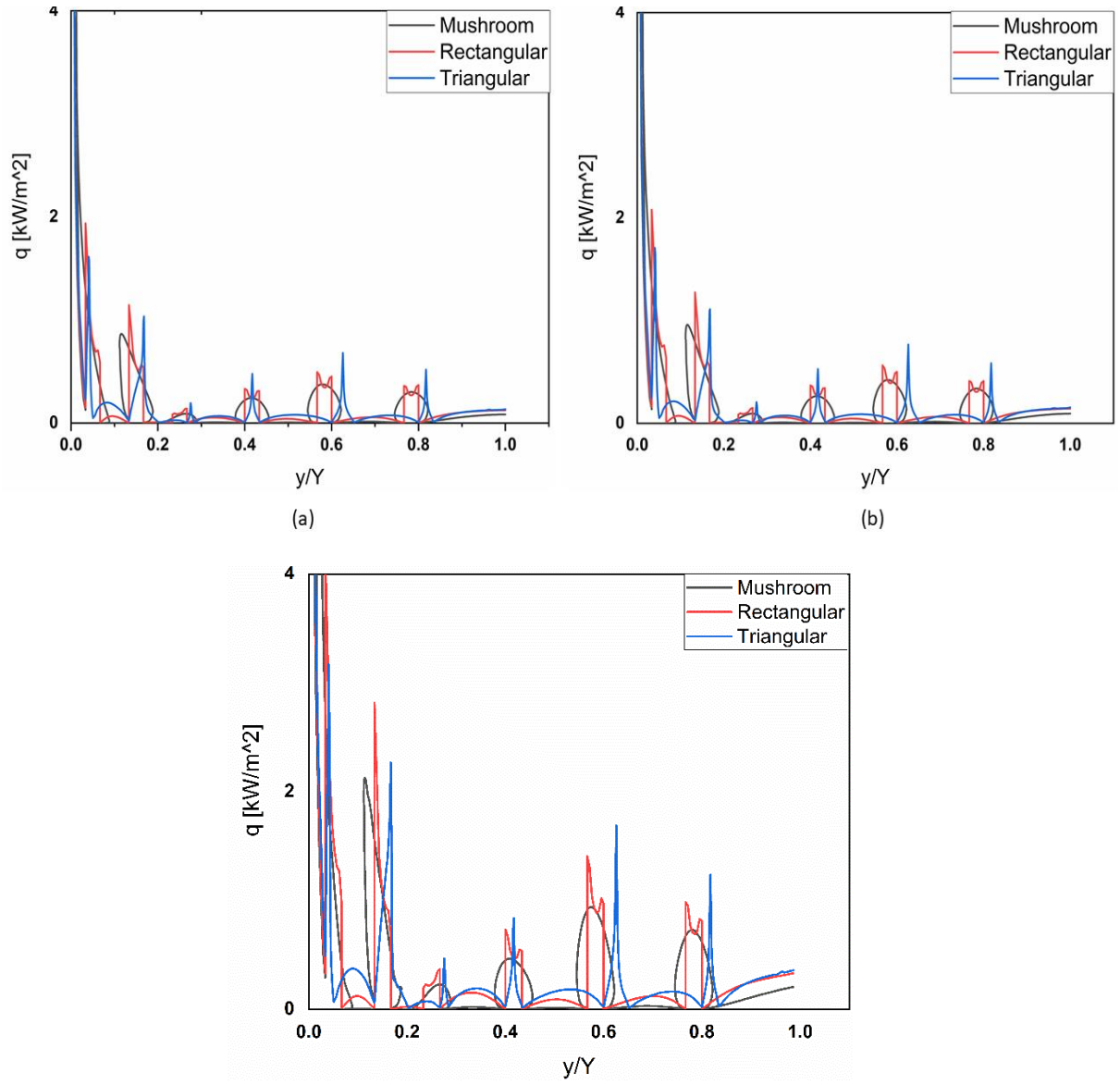

Fig (5.5.1): Comparison of wall heat flux of Mushroom shape of protrusion (For Left wall) with other shape for Re = 100 and (a) Pr = 0.7, (b) Pr = 1 & (c) Pr = 10.

In fig (5.5.1), we observe that for a particular Reynold's Number and Prandtl Number, wall heat flux is maximum for Mushroom shape of protrusions because it has maximum surface area and more blockage of fluid. But, as we increase the Prandtl Number, wall heat flux also increases because it reduces the thermal boundary layer thickness which allows more heat to transfer. Also, in graph we observe that area of heat transfer is maximum for Mushroom shape of protrusions. So, for a particular situation if our aim is to increases heat transfer from system then we must prefer Mushroom shape of protrusions at the walls.

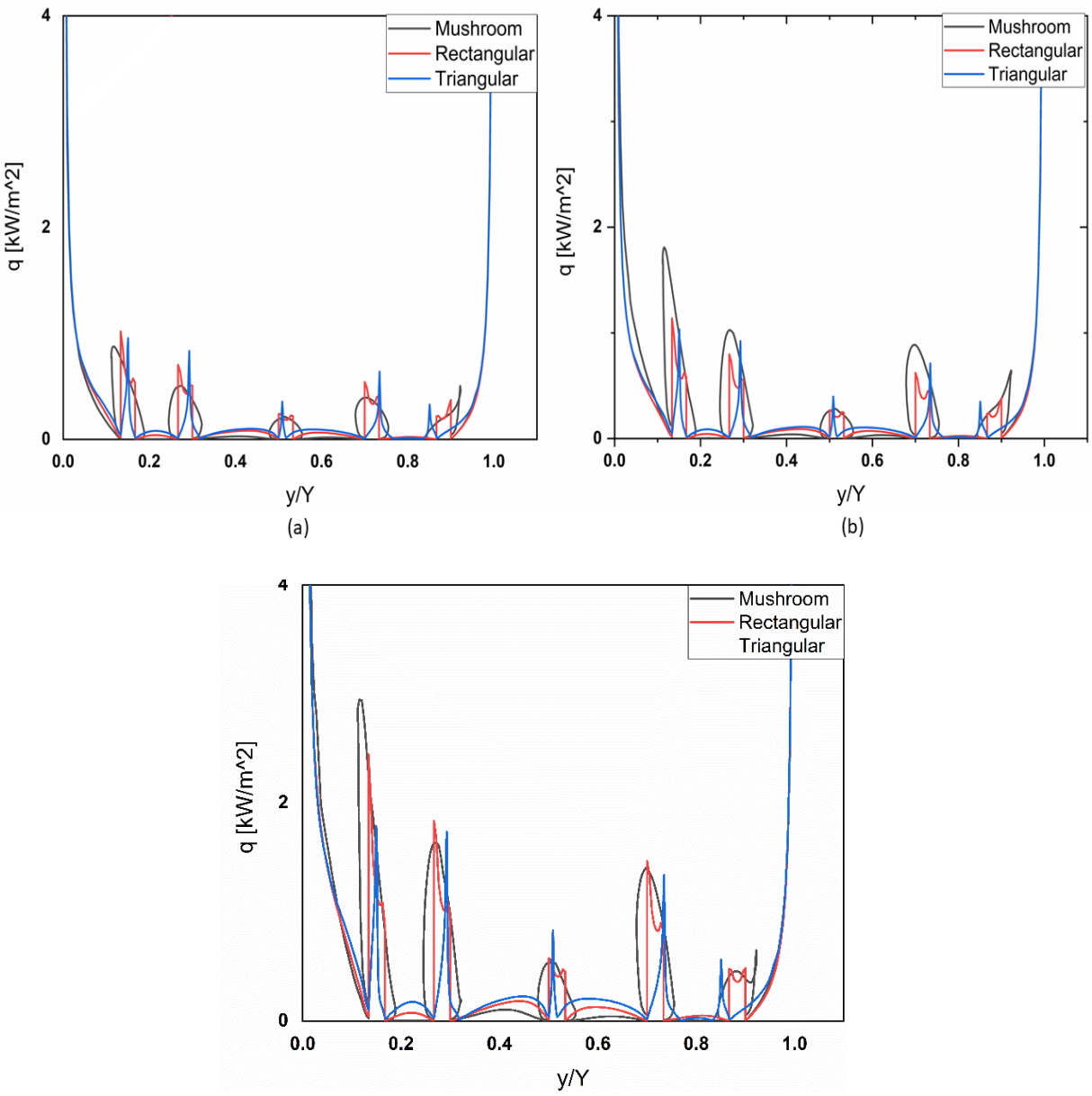

Fig (5.5.2): Comparison of wall heat flux of Mushroom shape of protrusion (For Right wall) with other shape for Re = 100 and (a) Pr = 0.7, (b) Pr = 1 & (c) Pr = 10.

In case of right wall, in fig (5.5.2) we observe that area of heat transfer is maximum for Mushroom shape of protrusions. For a particular Reynold's Number and Prandtl Number, wall heat flux is maximum for Mushroom shape of protrusions but it is less than respective protrusions of left wall in each case. On right wall, less protrusions are present which allows fluid to easily flow through the channel and less blockage so wall heat flux is less.

Chapter 6

Conclusion and Scope for future work

We have performed numerical modelling for mixed convection heat transfer in a vertical channel with varying shapes of protrusion at the walls of channel. Results are obtained for different values of Reynold's Number and Prandtl Numbers. Results are successfully validated through previous study of Laminar mixed convection flow in a vertical channel with single protrusion at wall as in the literature.

The following are the some of the main conclusion of this study:

- For a particular Reynold's Number as Prandtl Number increases (0.7 to 10), the value of h also increases for a particular shape of protrusions. The heat transfer rate increases with an increase in Reynolds number due to the increase in fluid velocity.

- At a plane near left wall, temperature rises upto first quarter due to blockage of fluid and after reaches maximum, it decreases. At a plane near right wall, it gradually increases and reaches maximum at outlet.

- For the Mushroom shape of protrusions, more heat transfer takes place which indicates less effect of buoyancy near the wall.

- In the first quarter of the channel near the left wall, q is more due to blockage of fluid and q is maximum for Mushroom Shape of protrusions.

- After the first quarter, as temperature start falling and there is formation of recirculation region so, Heat transfer also increases which is dependent on size and surface area of protrusions.

- Buoyancy significantly altered the flow and heat transfer characteristics in a vertical channel.

- A small recirculation zone forms at the inlet near the wall of the channel. The size of the recirculation zone increases and becomes maximum at middle wall.

References

[1] G. Madhusudhana Rao, G.S.V.L. Narasimham, Laminar conjugate mixed convection in a vertical channel with heat generating components. 2006.

[2] Antonio Barletta, Laminar mixed convection with viscous dissipation in a vertical channel, International Journal of Heat and Mass Transfer 41(1998) 3501-3513.

[3] P.M. Ligrani, G.I. Mahmood, J.L. Harrison, C.M. Clayton, D.L. Nelson, Flow structure and Nusslet number variations in a channel with dimples and protrusions on opposite walls, International Journal of Heat and Mass Transfer 44(2001) 4413-4425.

[4] C. Gururaja Rao, C. Balaji, S.P. Venkateshan, Effect of surface radiation on conjugate mixed convection in a vertical channel with a discrete heat source in each wall, International Journal of Heat and Mass Transfer 45 (2002) 3331–3347.

[5] A. Barletta , E. Magyari , B. Keller, Dual mixed convection flows in a vertical channel, International Journal of Heat and Mass Transfer 48 (2005) 4835–4845.

[6] Mohammad Hemmat Esfe, Ali Akbar Abbasian Arani, Amir Hossein Niroumand, Wei-Mon Yan, Arash Karimipour, Mixed convection heat transfer from surface-mounted block heat sources in a horizontal channel with nanofluids, International Journal of Heat and Mass Transfer 89(2015) 783-791.

[7] Enzo Zanchini, Efect of viscous dissipation on mixed convection in a vertical channel with boundary conditions of the third kind, International Journal of Heat and Mass Transfer 41 (1998) 3949-3959.

[8] J.C. Umavathi, M.S. Malashetty, Magnetohydrodynamic mixed convection in a vertical channel, International Journal of Non-Linear Mechanics 40 (2005) 91 – 101.

[9] W. Aung, G. Worku, Mixed convection in ducts with asymmetric wall heat fluxes, ASME J. Heat Transfer 109 (1987) 947–951

[10] C.H. Cheng, H.S. Huang, W.H. Huang, Flow reversal and heat transfer of fully developed mixed convection in vertical channels, J. Thermophys. Heat Transfer 4 (1990) 375–383

[11] T.T. Hamadah, R.A. Wirtz, Analysis of laminar fully developed mixed convection in a vertical channel with opposing buoyancy, ASME J. Heat Transfer 113 (1991) 507–510.

[12] Gilles Desrayaud, Alberto Fichera, Guy Lauriat, Natural convection air-cooling of a substrate-mounted protruding heat source in a stack of parallel boards, International Journal of Heat and Fluid Flow 28 (2007) 469-482.

[13] Bugra Sarper, Mehmet Saglam, Orhan Aydin, Experimental and numerical investigation of natural convection in a discretely heated vertical channel: Effect of the blockage ratio of the heat sources, International Journal of Heat and Fluid Flow 126 (2018) 894-910.

[14] S. Habchi and S. Acharya. (1986), Laminar mixed convection in a partially blocked, vertical channel, Int. J. Heat Mass Transfer, Vol. 29, No. 11, pp. 1711-1722,1986.

[15] Y. H. Hung and W. M. Shiau (1988), Local steady-state natural convention heat transfer in vertical parallel plates with a two-dimensional rectangular rib, Int. J. Heat Mass Transfer. Vol. 31, No. 6, pp. 1279-1288, 198.

[16] S.K. Mandal, Arnab Deb, Dipak Sen (2019), Mixed convective heat transfer with surface radiation in a rectangular channel with heat sources in presence of heat spreader, Thermal Engineering and Engineering Progress 14 (2019) 100423.

[17] Lyes Boutina, Rachid Bessaïh (2011), Numerical simulation of mixed convection air-cooling of electronic components mounted in an inclined channel, Applied Thermal Engineering 31 (2011) 2052-2062.

[18] G.I. Sultan (2000), Enhancing forced convection heat transfer from multiple protruding heat

sources simulating electronic components in a horizontal channel by passive cooling, Microelectronics Journal 31 (2000) 773–779.

[19] Giovanni Tandda (1996), Natural convection heat transfer in vertical channels with and without transverse square ribs, Int. J. Heat Mass Transfer. Vol. 40, No. 9, pp. 2173-2185, 1997.

[20] Kanchan M. Kelkar, Dipankar Choudhury (1993), Numerical prediction of periodically fully developed natural convection in a vertical channel with surface mounted heat generating blocks, Int. J. Heat Mass Transfer. Vol 36, No. 5, pp. 1133-1145, 1993.